JPRS L/8856

9 January 1980

USSR Report

EARTH SCIENCES

(FOUO 1/80)

FBIS FOREIGN BROADCAST INFORMATION SERVICE

APPROVED FOR RELEASE: 2007/02/08: CIA-RDP82-00850R000200040022-1

NOTE

JPRS publications contain information primarily from foreign newspapers, periodicals and books, but also from news agency transmissions and broadcasts. Materials from foreign-language sources are translated; those from English-language sources are transcribed or reprinted, with the original phrasing and other characteristics retained.

Headlines, editorial reports, and material enclosed in brackets [] are supplied by JPRS. Processing indicators such as [Text] or [Excerpt] in the first line of each item, or following the last line of a brief, indicate how the original information was processed. Where no processing indicator is given, the information was summarized or extracted.

Unfamiliar names rendered phonetically or transliterated are enclosed in parentheses. Words or names preceded by a question mark and enclosed in parentheses were not clear in the original but have been supplied as appropriate in context. Other unattributed parenthetical notes within the body of an item originate with the source. Times within items are as given by source.

The contents of this publication in no way represent the policies, views or attitudes of the U.S. Government.

For further information on report content call (703) 351-2938 (economic); 3468 (political, sociological, military); 2726 (life sciences); 2725 (physical sciences).

APPROVED FOR RELEASE: 2007/02/08: CIA-RDP82-00850R000200040022-1

JPRS L/8856

9 January 1980

USSR REPORT

EARTH SCIENCES

(FOUO 1/80)

CONTENTS PAGE

CONTENTS (Continued)

I. OCEANOGRAPHY

Translations

UDC 551.551

SIMILARITY RELATIONSHIP AND TURBULENCE SPECTRA IN STRATIFIED MEDIUM

Moscow IZVESTIYA AKADEMII NAUK SSSR, FIZIKA ATMOSFERY I OKEANA in Russian
Vol 15, No 8, 1979 pp 820-828

[Article by A. G. Sazontov, Institute of Applied Physics, submitted for publication 18 July 1978]

Abstract: A statistical description of turbulence in a temperature-stratified medium is considered on the basis of a characteristic functional. It is shown that the invariance of the equation for this functional relative to the group of scale transformations makes it possible to determine turbulence spectra in the buoyancy and inertial subintervals.

[Text] Turbulent motion in the ocean and atmosphere for the most part is determined by effects associated with the action of lift. The presence of temperature stratification exerts a considerable influence on the dynamics of turbulence and leads to qualitative differences in comparison with turbulence in a temperature-homogeneous medium. First, the predominance of a vertical direction leads to anisotropy in movements of all scales, and second, to a number of dimensional parameters there is added the parameter $g\beta$ (g is the acceleration of gravity, β is the coefficient of thermal expansion), which makes difficult an analysis associated with the use of the dimensionalities method. As is well known, in an unstratified medium in a broad range of wave numbers k a Kolmogorov spectrum $E_k \sim k^{-5/3}$ is established; this is obtained theoretically with use of the self-similarity hypothesis and locality hypothesis [1] and is confirmed quite well experimentally [2].

In a stratified medium the spectra are more complex. Experiments in the atmosphere and ocean show that there are several equilibrium scale intervals where the turbulence spectra have a different character. (A review of the theoretical and experimental results can be found in [3].)

As is well known [4], a full statistical description of the hydrodynamic fields of turbulent flow can be attained by stipulating a characteristic functional. The corresponding equation for turbulent motion, in which the

fluid is in the field of external forces, was obtained for an incompressible fluid in [5], for a compressible fluid -- in [6], and for a stratified fluid is obtained in this study.

It appears that in order to find the statistical characteristics of hydrodynamic fields it is not obligatory to know the explicit form of the solution for the characteristic functional; it is sufficient to determine the transformation properties of the corresponding equation relative to a group of scale transformations. For homogeneous isotropic turbulence such transformations and scaling properties were examined in the studies [7, 8] and for a compressible fluid in [6]. [In [7, 8], instead of a characteristic functional, use is made of the probability density in functional space, which can be regarded as a functional Fourier transform of the characteristic functional.] In this study it is demonstrated that the derived equation for the characteristic functional in a stratified medium allows a group of scale transformations which leads to the similarity theorem. The presence of this group (with the assumption of existence of sectors of equilibrium) makes it possible to find turbulence spectra in the inertial subinterval and the buoyancy subinterval.

Characteristic Functional of Stratified Fluid

In order to investigate the spectral structure of turbulence use is made of the equations of motion, continuity equation and thermal conductivity equation with external random forces in the Boussinesq approximation:

$$\frac{\partial u_i}{\partial t}+u_k\frac{\partial u_i}{\partial x_k}=-\frac{\partial p'}{\partial x_i}+g\beta\theta\lambda_i+\nu\Delta u_i+f_i(x,t), \tag{1}$$

$$\frac{\partial\theta}{\partial t}+u_k\frac{\partial\theta}{\partial x_k}=\frac{\partial\bar{T}}{\partial z}u_j\lambda_j+\varkappa\Delta\theta+q(x,t), \tag{2}$$

$$\frac{\partial u_i}{\partial x_i}=0. \tag{3}$$

where x_i are Cartesian coordinates (x_3 is the vertical coordinate); t is time; u_i are velocity components; p', θ are the deviations of pressure and temperature from the standard hydrostatic values; ν is the coefficient of molecular heat conductivity; $g\beta$ is the buoyancy parameter; $\partial\bar{T}/\partial z$ is the mean constant temperature gradient; λ is a unit vector with the components $\lambda = (0, 0, 1)$.

In the considered model the kinetic energy of the fluid and temperature are maintained due to the operation of external forces; the random forces model the fluctuations of averaged flow, accomplishing pumping of energy to large-scale pulsations. We will assume that $f_i(x, t)$ and $q(x, t)$ are Gaussian, homogeneous and delta-correlated with time with a mean value equal to zero

$$\begin{gathered}\langle f_i(\mathbf{x}, t)\rangle=\langle q(\mathbf{x}, t)\rangle=0, \\ \langle f_i(\mathbf{x}_1 t_1) f_j(\mathbf{x}_2, t_2)\rangle=B_{ij}(\mathbf{x}_2-\mathbf{x}_1)\delta(t_2-t_1), \\ \langle q(\mathbf{x}_1, t_1) q(\mathbf{x}_2, t_2)\rangle=G(\mathbf{x}_2-\mathbf{x}_1)\delta(t_2-t_1).\end{gathered} \tag{4}$$

The statistical properties of the hydrodynamic velocity and temperature fields will be described by the characteristic functional

$$\Phi=\left\langle \exp i \int_{-\infty}^{\infty}\{y_i(\mathbf{x}) u_i(\mathbf{x}, t)+z(\mathbf{x})\theta(\mathbf{x}, t)\} d^3x \right\rangle, \tag{5}$$

where $y_i(x)$ and $z(x)$ are sufficiently smooth (for example, continuous or continuous and differentiable a definite number of times) arbitrary functions.

The averaging in (5) is carried out on the basis of the distribution probability of external forces. It follows from equation (3) that

$$\Phi\{y(\mathbf{x})+\nabla\psi;\ z(\mathbf{x})\}=\Phi\{y(\mathbf{x});\ z(\mathbf{x})\}, \tag{6}$$

where ψ is an arbitrary function whose gradient sufficiently rapidly tends to zero at infinity. As a result of (6) we take into account the solenoidality of the vector field y(x). Differentiating (5) in time and taking into account the motions (1)-(3), for Φ we obtain the following equation in variational derivatives:

$$\begin{gathered}\frac{\partial \Phi}{\partial t}=i \int_{-\infty}^{\infty} y_i(\mathbf{x})\left\{D_k \frac{\partial}{\partial x_k} D_i+ig\beta\lambda_i D_\theta-i\nu\Delta D_i\right\}\Phi\, d^3x+ \\ +i \int_{-\infty}^{\infty} z(\mathbf{x})\left\{D_k \frac{\partial}{\partial x_k} D_\theta+i\tilde{a}\lambda_j D_j-i\varkappa\Delta D_\theta\right\}\Phi\, d^3x+I, \\ D_i=\frac{\delta}{\delta y_i(\mathbf{x}) d^3\mathbf{x}}, \quad D_\theta=\frac{\delta}{\delta z(\mathbf{x}) d^3\mathbf{x}}.\end{gathered} \tag{7}$$

Here Di and D_0 are operators of variational differentiation; I is a source describing the influence of the external forces on the fluid

$$\begin{gathered}I=-\int_{-\infty}^{\infty}\left\{y_i(\mathbf{x})\left\langle f_i(\mathbf{x}, t)\exp i \int_{-\infty}^{\infty}(y_k u_k+z\theta) d^3\mathbf{x}\right\rangle+\right. \\ \left.+z(\mathbf{x})\left\langle q(\mathbf{x}, t)\exp i \int_{-\infty}^{\infty}(y_k u_k+z\theta) d^3\mathbf{x}\right\rangle\right\} d^3\mathbf{x}.\end{gathered} \tag{8}$$

As a result of the solenoidality of the vector field y(x) the term corresponding to pressure does not enter into equation (7).

We will assume that the forces became operative at the time t = 0; when t = 0 the fluid is assumed to be at rest:

$$\begin{gathered}\mathbf{u}|_{t=0}=0|_{t=0}=0, \quad \text{that is,} \\ \Phi|_{t=0}=1.\end{gathered} \tag{9}$$

Equation (7) with the initial condition (9) is the Cauchy problem for the characteristic functional in a temperature-stratified medium.

For Gaussian, time delta-correlated random forces it is easy to express the source I through Φ

$$I = -\frac{1}{2}\int\int_{-\infty}^{\infty} y_i(\mathbf{x})\, y_j(\mathbf{x}_1) B_{ij}(\mathbf{x}-\mathbf{x}_1)\, d^3\mathbf{x}\, d^3\mathbf{x}_1 - \\ -\frac{1}{2}\int\int_{-\infty}^{\infty} z(\mathbf{x})\, z(\mathbf{x}_1) G(\mathbf{x}-\mathbf{x}_1)\, d^3\mathbf{x}\, d^3\mathbf{x}_1\, \Phi. \tag{10}$$

It can be interpreted as a term responsible for "diffusion in velocity and temperature space." It is possible to find restrictions on the diffusion coefficients B_{ij} and G; these restrictions are imposed by the stationarity conditions. In actuality, in this model the stationary temperature regime is maintained due to the operation of external forces. By averaging the equation for the balance of energy in the fluid and the temperature inhomogeneity $1/2\,\theta^2$, on the basis of external forces we obtain

$$\langle f_i u_i \rangle = 2\nu \left\langle \left(\frac{\partial u_i}{\partial x_i}\right)^2 \right\rangle - g\beta \langle \theta u_3 \rangle, \tag{11}$$

$$\langle q\theta \rangle = 2\varkappa \left\langle \left(\frac{\partial \theta}{\partial x_j}\right)^2 \right\rangle - \frac{\partial \overline{T}}{\partial z} \langle \theta u_3 \rangle. \tag{12}$$

The left-hand sides of formulas (11) and (12) can be expressed through the corresponding correlators of external forces using the Furutsu-Novikov formula

$$\langle f_i u_i \rangle = \int\int_{-\infty}^{\infty} \langle f_i(\mathbf{x}, t) f_j(\mathbf{x}_1, t_1) \rangle \left\langle \frac{\delta u_i(\mathbf{x}, t)}{\delta f_j(\mathbf{x}_1, t) d\mathbf{x}_1\, dt} \right\rangle d\mathbf{x}_1\, dt,$$

$$\langle q\theta \rangle = \int\int_{-\infty}^{\infty} \langle q(\mathbf{x}, t) q(\mathbf{x}_1, t_1) \rangle \left\langle \frac{\delta \theta(\mathbf{x}, t)}{\delta q(\mathbf{x}_1, t) d\mathbf{x}_1\, dt} \right\rangle d\mathbf{x}_1\, dt.$$

Using the relationships

$$\frac{\delta u_i(\mathbf{x}, t)}{\delta f_j(\mathbf{x}_1, t) d\mathbf{x}_1\, dt} = \frac{1}{2}\delta_{ij}\delta(\mathbf{x}-\mathbf{x}_1), \qquad \frac{\delta \theta(\mathbf{x}, t)}{\delta q(\mathbf{x}_1, t) d\mathbf{x}_1\, dt} = \frac{1}{2}\delta(\mathbf{x}-\mathbf{x}_1),$$

from (11) and (12) we obtain

$$\frac{1}{2} B_{ii}(0) = \varepsilon - g\beta \langle \theta u_3 \rangle, \qquad \frac{1}{2} G(0) = \varepsilon_T - \frac{\partial \overline{T}}{\partial z} \langle \theta u_3 \rangle, \tag{13}$$

$\varepsilon = \nu \langle (\partial u / \partial x_j)^2 \rangle$ is the mean dissipation rate; $\varepsilon_T = \varkappa \langle (\partial \theta / \partial x_j)^2 \rangle$ is the mean rate of dissipation of temperature inhomogeneities; $g\beta \langle \theta u_3 \rangle$ is the mean work of Archimedes force in turbulent movements of fluid elements.

Using (13), it is possible to write the correlators of external forces in the following way:

$$B_{ij}(\mathbf{r}) = 2[\varepsilon - g\beta\langle 0u_3\rangle]b_{ij}, \quad G(\mathbf{r}) = 2\left[\varepsilon_T - \frac{\partial \bar{T}}{\partial z}\langle 0u_3\rangle\right]\bar{g}\left(\frac{\mathbf{r}}{L_T}\right), \tag{14}$$

where b_{ij} is a dimensionless tensor, on the assumption of only homogeneity of the random force having six independent components with the characteristic scales $L_1, L_2, \ldots, L_6$; $b_{ii}(0) = 1$; $\bar{g}$ is a dimensionless function having the characteristic scale L_T.

The detailed structure of the tensor b_{ij} and the function $\bar{g}$ for our purposes is unimportant.

Equation (7) with the source (10) and the initial condition (9) are invariant relative to the following group of transformations:

$$\begin{gathered}
\alpha\mathbf{x}=\mathbf{x}', \ \alpha^{1-\gamma}t=t', \ \alpha^{(\gamma+3)}\mathbf{y}(\mathbf{x})=\mathbf{y}'(\mathbf{x}'), \\
\alpha^{(\delta+3)}z(\mathbf{x})=z'(\mathbf{x}'), \ \alpha^{1+\gamma}\nu=\nu', \ \alpha^{1+\gamma}\varkappa=\varkappa', \\
\alpha^{3\gamma-1}B_{ij}=B_{ij}', \ \alpha^{2\delta+\gamma-1}G=G', \ \alpha^{2\gamma-\delta-1}g\beta=(g\beta)', \\
\alpha^{\delta-1}\frac{\partial\bar{T}}{\partial z}=\frac{\partial\bar{T}'}{\partial z}, \quad \alpha^{3\gamma-1}\varepsilon=\varepsilon', \quad \alpha^{2\delta+\gamma-1}\varepsilon_T=\varepsilon_T', \quad \alpha L_T=L_T', \quad \alpha L=L',
\end{gathered} \tag{15}$$

where L is the general external turbulence scale; $L = \min(L_1, L_2, \ldots, L_6)$; α, γ, δ are derivative parameters. Hence from the uniqueness of solution of the Cauchy problem for equation (7) we have the similarity theorem:

$$\begin{gathered}
\Phi\left\{\mathbf{y}(\mathbf{x}), z(\mathbf{x}), t, \varepsilon, \varepsilon_T, \frac{\partial\bar{T}}{\partial z}, g\beta, \nu, \varkappa, L, L_T\right\} = \\
= \Phi\{\mathbf{y}'(\mathbf{x}'), z'(\mathbf{x}'), t', \varepsilon', \varepsilon_T', \bar{\alpha}', (g\beta)', \nu', \varkappa', L', L_T'\}.
\end{gathered} \tag{16}$$

We note that in contrast to the similarity hypotheses (16) represents a precise relationship.

Our objective is to use this property for obtaining information on the correlation functions which are generated by the Φ functional.

Henceforth the external turbulence scales L and L_T tend to infinity and we will also limit ourselves to an examination of sufficiently small-scale pulsations. In this case the probability distribution of turbulent pulsations is not dependent on the dissipative parameters and initial characteristics of the flow. It can be demonstrated that the neglecting of dissipative factors is legitimate for scales $k \ll 1/\eta$, $1/\eta_T$, where $\eta = \nu^{3/4}/\bar{\varepsilon}^{1/4}$ and $\eta_T = \varkappa^{3/4}/\bar{\varepsilon}^{1/4}$ are the Kolmogorov internal turbulence scales for the velocity and temperature fields.

Turbulence Spectra in Inertial Subinterval and in Buoyancy Subinterval

Now we will proceed to computation of the turbulence spectra similar to [6]. We will examine the special case when in the medium there is no mean temperature gradient, that is, $\partial \overline{T}/\partial z = 0$.

We will examine the kinetic energy spectrum

$$E(k) = -\frac{1}{(2\pi)^3} \iint_{|\mathbf{k}|=k} \int_{-\infty}^{\infty} e^{-i\mathbf{k}\mathbf{x}} \{D_i D_i \Phi\}_{y=z=0} \, d^3x \, dS(\mathbf{k}), \tag{17}$$

where $dS(k)$ is an element of sphere surface area $|k| = k$.

Using (16), in (17) we convert to the functional of the variables with primes and assuming that $\alpha = k$, we obtain

$$E(k) = \frac{f(k^{3\gamma-1}\varepsilon; k^{2\delta+\gamma-1}\varepsilon_\tau; k^{2\gamma-\delta-1}g\beta; k^{1-\gamma}t)}{k^{2\gamma+1}}.$$

In a stationary case $\partial E/\partial t = 0$ from the arbitrariness of γ and δ it follows that $\partial E/\partial\delta = 0$ and $\partial E/\partial\gamma = 0$.

From the condition $\partial E/\partial\delta = 0$ we obtain the equation

$$2\xi_1 \frac{\partial f}{\partial \xi_1} - \xi_2 \frac{\partial f}{\partial \xi_2} = 0,$$

$$\xi_1 = k^{2\delta+\gamma-1}\varepsilon_\tau, \quad \xi_2 = k^{2\gamma-\delta-1}g\beta,$$

whose solution is

$$f = f(k^{3\gamma-1}\varepsilon; \xi_1^{1/2}\xi_2) \equiv f(k^{3\gamma-1}\varepsilon; g\beta\varepsilon_\tau^{1/2}k^{5\gamma/2-1/2});$$

from the condition $\partial E/\partial\gamma = 0$ it follows that

$$3\zeta_1 \frac{\partial f_1}{\partial \zeta_1} + \frac{5}{2}\zeta_2 \frac{\partial f_1}{\partial \zeta_2} = 2f_1,$$

where

$$\zeta_1 = k^{3\gamma-1}\varepsilon, \quad \zeta_2 = g\beta\varepsilon_\tau^{1/2}k^{5\gamma/2-1/2}$$

hence

$$f_1 = \zeta_1^{2/3}\Psi(\zeta_1^{6/5}/\zeta_2^3).$$

As a result, the spectral density of kinetic energy has the form

$$E(k) = \varepsilon^{-2/3}k^{-5/3}\Psi((kL_*)^2), \tag{18}$$

where

$$L_* = \varepsilon^{3/4}/(g\beta)^{3/4}\varepsilon_\tau^{3/4}$$

is the scale characterizing the minimum dimension of the inhomogeneities from which the influence of buoyancy becomes significant. This scale was introduced independently by A. M. Obukhov [9] and Boldgiano [10].

Similarly, for the temperature field spectrum

$$E_{TT}(k) = -\frac{1}{(2\pi)^3}\iint\limits_{|\mathbf{k}|=k}\int\limits_{-\infty}^{\infty} e^{-i\mathbf{kx}}\{D_0 D_\theta \Phi\}_{y=z=0}\, d^3\mathbf{x}\, dS(\mathbf{k})$$

and the reciprocal spectral density of temperature and vertical velocity

$$E_{TW}(k) = -\frac{1}{(2\pi)^3}\iint\limits_{|\mathbf{k}|=k}\int\limits_{-\infty}^{\infty} e^{-i\mathbf{kx}}\{\lambda_j D_j D_\theta \varphi\}_{y=z=0}\, d^3\mathbf{x}\, dS(\mathbf{k})$$

it is possible to obtain the following expressions:

$$E_{TT}(k) = \frac{f_{TT}(k^{3\tau-1}\varepsilon, k^{2\delta+\tau-1}\varepsilon_\tau, k^{2\tau-\delta-1}g\beta; k^{1-\tau}t)}{k^{2\delta+1}}$$

$$E_{TW}(k) = \frac{f_{TW}(k^{3\tau-1}\varepsilon, k^{2\delta+\tau-1}\varepsilon_\tau, k^{2\tau-\delta-1}g\beta, k^{1-\tau}t)}{k^{\delta+\tau+1}},$$

or

$$E_{TT}(k) = \varepsilon_\tau \varepsilon^{1/3} k^{-5/3}\Psi_{TT}(kL_*), \tag{19}$$

$$E_{TW}(k) = \varepsilon_\tau \varepsilon^{1/3} k^{-5/3}\Psi_{TW}(kL_*). \tag{20}$$

We note that when obtaining the spectra (18-20) it is not necessary to make any assumptions concerning the nature of energy transfer in the spectrum. In the absence of gravity, causing stratification (that is, when $g\beta = 0$), formulas (18)-(20) must be transformed into the ordinary formulas of locally isotropic turbulence of an unstratified fluid. But when $g\beta \to 0$, $L_* \to \infty$, and accordingly there must be satisfaction of the conditions $\Psi(\infty) = \Psi_{TT}(\infty) = 1$ and $\Psi_{TW}(\infty) = 0$. Thus, if $k \gg L_*^{-1}$, the values of the correction functions in formulas (18)-(20) can be replaced by their values at infinity.

The invariance of the equation for the characteristic functional relative to the group (17) imposes singular restrictions on the functional dependences of the spectral characteristics. But these restrictions still leave a great arbitrariness of the functional type. This circumstance is entirely natural because the corresponding invariance is a reflection of the singular self-similarity of the spectral characteristics following from (18). It is clear that in itself expression (18) does not contain any dynamic information. Therefore, in order to obtain specific information on the spectral functions it is necessary to have additional information. Such information can be drawn either from the theory of perturbations or from physical assumptions as to what parameters are decisive in the corresponding interval of scales.

Since the use of the theory of perturbations for equation (7) meets with considerable difficulties due to the absence of a suitable zero approximation, when finding the turbulence spectra in the buoyancy interval we make use of the Boldgiano physical hypothesis [10], which involves the following. With $k \gg L_*^{-1}$ in the case of a stable stratification the energy received in the considered interval is expended to a considerable degree on work against buoyancy forces and only an insignificant part goes to small-scale perturbations, where viscous dissipation is important. It can therefore be hoped

that in the region $k \ll L_*^{-1}$ the $\bar{\varepsilon}$ parameter will exert little influence on the form of the turbulence spectra and in this case we have the characteristic functional

$$\Phi = \Phi\{\mathbf{y}, z, \varepsilon_\tau, g\beta, t\}. \tag{21}$$

Whereas at the depth of the inertial interval it is usually assumed that the turbulence is isotropic despite an anisotropic nature of its excitation and the presence of stratification, in the buoyancy subinterval the hydrodynamic turbulence fields are essentially locally axially symmetric (that is, locally homogeneous in all directions and locally isotropic horizontally). In the investigation of their local three-dimensional structure we make use of the circumstance that in the absence of dissipative parameters the formulation of the problem allows a broader group of transformations. Specifically, we will measure the scale in different units in the direction z and the scales in horizontal directions:

$$\alpha_z z = z', \ \alpha_\perp \mathbf{r}_\perp = \mathbf{r}_\perp'.$$

In this case equation (7) with $\nu = \varkappa = 0$ and the initial condition (9) will be invariant relative to the group:

$$\begin{gathered}
\alpha_z \alpha_\perp^{\gamma} t = t', \quad \alpha_\perp^{-(\gamma+3)} y_{1,2}(\mathbf{x}) = y_{1,2}'(\mathbf{x}'), \\
\alpha_z^{-1} \alpha_\perp^{-(\gamma+2)} y_3(\mathbf{x}) = y_3'(\mathbf{x}'), \quad \alpha_z^{-\eta} \alpha_\perp^{-(\delta+3)} z(\mathbf{x}) = z'(\mathbf{x}'), \\
\alpha_z^{\eta} \alpha_\perp^{2\gamma-\delta-1} g\beta = (g\beta)', \quad \alpha_z^{\eta-2} \alpha_\perp^{\delta+1} \frac{\partial T}{\partial z} = \frac{\partial T'}{\partial z}, \\
\alpha_z^{2\eta-3} \alpha_\perp^{\gamma+2\delta+2} G = G', \quad \alpha_z^{-3} \alpha_\perp^{3\gamma+2} B_{\alpha\beta} = B_{\alpha\beta}' \quad (\alpha, \beta = 1, 2), \\
\alpha_z^{-2} \alpha_\perp^{3\gamma+1} B_{\alpha 3} = B_{\alpha 3}', \quad \alpha_z^{-1} \alpha_\perp^{3\gamma} B_{33} = B_{33}', \\
\alpha_z^{2\eta-3} \alpha_\perp^{\gamma+2\delta+2} \varepsilon_\tau = \varepsilon_\tau',
\end{gathered} \tag{22}$$

where α_z, $\alpha_\perp$, γ, δ, η are arbitrary parameters.

The group of transformations (22) is broader than the similarity transformation group for values with independent dimensionalities, as is the case for (16). The similarity theorem following from (22)

$$\begin{aligned}
&\Phi\left\{y_{1,2}(\mathbf{x}), y_3(\mathbf{x}), z(\mathbf{x}), t, \varepsilon_\tau, \frac{\partial \bar{T}}{\partial z}, g\beta\right\} = \\
&= \Phi\left\{y_{1,2}'(\mathbf{x}'), y_3'(\mathbf{x}'), z'(\mathbf{x}'), t', \varepsilon_\tau', \frac{\partial \bar{T}'}{\partial z}, g\beta'\right\}
\end{aligned} \tag{23}$$

makes it possible to determine the anisotropic spectral characteristics in the buoyancy subinterval.

For the spectral characteristics of interest to us, using (23), in a case when the influence of the mean temperature gradient is insignificant, we have

$$F(k_z, k_\perp) = \frac{k^2 f(k_z^{2\eta-3} k_\perp^{\gamma+2\delta+2} \varepsilon_\tau; k_z^{-\eta} k_\perp^{2\gamma-\delta-1} g\beta)}{k_z k_\perp^{2\gamma+4}},$$

$$F_{TT}(k_z, k_\perp) = \frac{f_{TT}(k_z^{2\eta-3} k_\perp^{\gamma+2\delta+2} \varepsilon_\tau; k_z^{-\eta} k_\perp^{2\gamma+\delta-1} g\beta)}{k_z^{2\eta-1} k_\perp^{2\delta+4}},$$

$$F_{TW}(k_z, k_\perp) = \frac{f_{TW}(k_z^{2\eta-3} k_\perp^{\gamma+2\delta+2} \varepsilon_\tau; k_z^{-\eta} k_\perp^{2\gamma-\delta-1} g\beta)}{k_z^{\eta} k_\perp^{\gamma+\delta+3}} \quad (k^2 = k_z^2 + k_\perp^2),$$

hence, by a standard method we obtain

$$\begin{aligned} F(k_z, k_\perp) &= C_1 \varepsilon_\tau^{2/3} (g\beta)^{4/3} k^2 k_z^{-11/3} k_\perp^{-4}, \\ F_{TT}(k_z, k_\perp) &= C_2 \varepsilon_\tau^{4/3} (g\beta)^{-2/3} k_z^{-7/3} k_\perp^{-2}, \\ F_{TW}(k_z, k_\perp) &= C_3 \varepsilon_\tau^{2/3} (g\beta)^{1/3} k_z^{-8/3} k_\perp^{-2}. \end{aligned} \tag{24}$$

Thus, the spectra in the buoyancy subinterval can be found if one adopts the unique physical hypothesis that in the interval $k \ll L^{-1}$ the $\bar{\varepsilon}$ parameter exerts little influence on the statistical characteristics. We note that such a hypothesis, together with dimensionality considerations, also gives an explicit form of the spectra, but it is important that dimensionality considerations can give only averaged spectra (Boldgiano-Monin spectra), whereas the presence of group (22) makes it possible to find anisotropic spectral distributions. In the presence of a mean temperature gradient $\partial \bar{T}/\partial z$ is added to the determining parameters. In this case in the buoyancy subinterval $\Phi = \Phi\{y, z, t, \varepsilon_T, \partial \bar{T}/\partial z, g\beta\}$. Using group (22), by the standard method we obtain the following expression for the spectral characteristics:

$$\begin{aligned} F(k_z, k_\perp) &= \frac{\partial \bar{T}}{\partial z} g\beta k^2 k_z^{-3} k_\perp^{-4} \Psi(k_z L_0^*), \\ F_{TT}(k_z, k_\perp) &= \left(\frac{\partial \bar{T}}{\partial z}\right)^2 k_z^{-3} k_\perp^{-2} \Psi_{TT}(k_z L_0^*), \\ F_{TW}(k_z, k_\perp) &= \left(\frac{\partial \bar{T}}{\partial z}\right)^{1/2} (g\beta)^{1/2} k_z^{-3} k_\perp^{-2} \Psi_{TW}(k_z L_0^*). \end{aligned} \tag{25}$$

Here $$L_0^* = \varepsilon_\tau^{1/2} / (g\beta)^{1/2} \left(\frac{\partial \bar{T}}{\partial z}\right)^{3/4}$$

is the scale characterizing the minimum dimension of the inhomogeneities, where the influence of the characteristics of the averaged temperature field becomes important. We note that the spectra (25), averaged by angles, lead to the known Schur-Lamly result.

It can be shown that (24) and (25) are noncontradictory. In actuality, with highly stable stratification in the buoyancy interval there is satisfaction of the condition

$$\varepsilon \ll g\beta\varepsilon_\tau \Big/ \frac{\partial \bar{T}}{\partial z}$$

Since the scales L_* and L_0^* are related by the expression

$$L_* = L_0^* \left(\frac{\frac{\partial \bar{T}}{\partial z}\varepsilon}{g\beta\varepsilon_\tau} \right)^{3/4},$$

the L_* scale is always less than L_0^* and in the interval of scales $L_0^* \gg L_*$ the spectra (24) are obtained when $k^{-1} \gg L_0^*$, that is (25). The width of these intervals in each specific case is determined by the ratio

$$\frac{\partial \bar{T}}{\partial z}\varepsilon \Big/ g\beta\varepsilon_\tau,$$

and in an experiment it is possible to encounter sectors of wave numbers corresponding to each of these spectra.

In conclusion the author expresses appreciation to M. I. Rabinovich for interest in the work, M. A. Rayevskiy for valuable comments, and also V. V. Kurin and Ye. I. Yakubovich for productive discussions.

BIBLIOGRAPHY

1. Kolmogorov, A. N., "Local Structure of Turbulence in Incompressible Fluid in Cases of Very Large Reynolds Numbers," DOKL. AN SSSR (Reports of the USSR Academy of Sciences), 30, No 4, pp 299-302, 1941.

2. Monin, A. S., Yaglom, A. M., STATISTICHESKAYA GIDROMEKHANIKA (Statistical Hydromechanics), Parts I and II, "Nauka," 1965, 1967.

3. FIZIKA OKEANA (Ocean Physics), Vol 1, edited by A. S. Monin, "Nauka," 1978.

4. Hopf, E., "Statistical Hydromechanics and Functional Calculus," J. RAT. MECH. ANAL., 1, No 1, 87, 1952.

5. Novikov, Ye. A., "Functionals and Random Forces Method in Turbulence Theory," ZhETF (Journal of Experimental and Technical Physics), 47, No 5(11), 1919-1926, 1964.

6. Moiseyev, S. S., Tur, A. V., Yanovskiy, V. V., "On the Theory of Strong Turbulence," PREPRINT KhFTI (Preprint of the Khar'kov Physical and Technical Institute), 76-41, Khar'kov, 1976; ZhETF, 71, No 9, 1976.

7. Nelkin, M., "Intermittency in Fully Developed Turbulence as a Consequence of the Navier-Stokes Equation," PHYS. REV. LETT., 30, No 21, 1029, 1973.

8. Nelkin, M., "Turbulence, Critical Fluctuations and Intermittency," PHYS. REV., A9, No 1, 388, 1974.

9. Obukhov, A. M., "Influence of Archimedes Forces on Structure of the Temperature Field in a Turbulent Flow," DOKL. AN SSSR, 125, No 5, 1959.

10. Boldgiano, R., "Turbulent Spectra in a Stably Stratified Atmosphere," JGR, 64, No 4, 1959.

11. Lin, I. T., Panchev, S., Cermak, J. E., "A Modified Hypothesis on Turbulence Spectra in the Buoyancy Subrange of Stably Stratified Shear Flow," RADIO SCI., 4, No 12, 1333, 1969.

[19-5303]

5303
CSO: 1866

UDC 551.465.73

EFFECT OF SURFACE WAVES ON HEAT EXCHANGE BETWEEN THE OCEAN AND ATMOSPHERE

Moscow IZVESTIYA AKADEMII NAUK SSSR, FIZIKA ATMOSFERY I OKEANA in Russian
Vol 15, No 9, 1979 pp 953-963

[Article by G. S. Dvoryaninov, Marine Hydrophysics Institute, Ukrainian Academy of Sciences, submitted for publication 19 June 1978, after revision 25 December 1978]

Abstract: The effect of the thin sur ace temperature boundary layer in the process of heat exchange between the atmosphere and ocean is evaluated when surface waves are present. It is shown that allowance for the existence of a warm film at the ocean surface gives a considerably greater increase in the heat flow through the discontinuity caused by waves in comparison with a case when the film effect is not taken into account. The author formulates the problem of wave transfer of heat, on the basis of whose solution the conclusion is drawn that the wave transfer mechanism, being a consequence of the nonpotentiality and nonlinearity of the waves, can be responsible for an increase in the heat flow through the warm film.

[Text] The ocean surface has a fundamental property -- the presence of a thin warm sublayer (warm film 0 (1 mm)) with large vertical gradients of the thermodynamic characteristics of the medium. The temperature difference within the limits of this sublayer has the value 0.4-2° [1-6], which causes a considerable vertical heat flow. Recently investigations have been made [5-8] which have given increased attention to the structure of the warm film (WF). The experiments in [2-9] gave the following principal results: 1) the WF is stable relative to the wind effect and is not destroyed if its velocity is less than 10 m/sec; 2) the thickness of the WF decreases with the development of wind waves and is dependent on the phase of the waves at a particular point in space; 3) the temperature change outside the layer attenuates exponentially and heat transfer

in it occurs by means of the molecular diffusion mechanism, so that the total heat flow is

$$q_x = -\varkappa \operatorname{grad} T(\eta)\,|_{\eta=0}, \tag{1.1}$$

where $\varkappa$ is the coefficient of molecular diffusion of heat in water; $T(\eta)$ is temperature; η is the coordinate normal to the surface, directed within the fluid.

2. It was demonstrated in [10] that an increase in heat exchange between the atmosphere and ocean due to the mean increment in surface area attributable to waves is not more than 15% in the case of adequately strong wave action (mean square wave steepness ~ 0.5). But in the presence of a warm film the waves will lead not only to an increase in the area of the discontinuity, but also to a decrease in the thickness of the film, that is, to a decrease in the path of heat diffusion and an increase in the temperature gradient along the normal to the ocean surface, which can substantially intensify heat exchange between the atmosphere and ocean in comparison with the undisturbed surface. This matter was studied theoretically in [11]. However, the condition of potentiality of motion, which was proposed in that study, requires that the averaged heat flow $\widetilde{T}\widetilde{\omega}$, caused by the correlations between the velocity and temperature wave fields, be absent. At the same time, the experiments reported in [12] indicate that it can be significant. In addition, the author of [11] presented an analysis for cases when either the temperature difference between the discontinuity and the lower boundary of the film or the heat flow through the WF were held constant for waves of different amplitude. But waves deform the temperature field and the film itself and therefore these conditions can be maintained only artificially. At the same time, this requirement and the constancy of temperature at the lower boundary of the film, adopted in [11], have this result: the temperature of the water surface must remain constant.

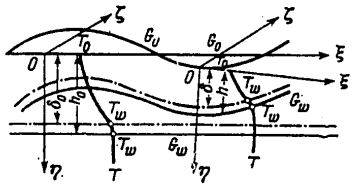

Fig. 1. Diagram of temperature boundary layer.

In this study, in the evaluation of the influence of waves on heat diffusion, there is no requirement for potentiality of the wave field and no restrictions are placed on the temperature field. However, temperature fluctuations along the wave are computed. Here use is made of the experimentally checked [7] correlation between the thickness of the temperature

boundary layer and the temperature difference at its boundaries; the general relationships are derived for three-dimensional waves. We will also consider the mechanism of generation of wave heat fluxes, governed by the viscosity and nonlinearity of wave movement.

Assume that an orthogonal curvilinear coordinate system ξ, ζ, η is placed at the ocean surface in such a way that ξ, ζ lie at the surface and η coincides with the internal normal to it. There is no precise lower boundary of the WF and therefore in the water we select some fictitious surface G_w (Fig. 1), which in the absence of waves is parallel to the ocean surface G_0 and is situated beneath it at the short distance h in such a way that $h \approx \delta$, but $h \geqslant \delta$, where δ is the thickness of the WF. Thus, the film will be situated within the region bounded by the surfaces G_0 and G_w, and its lower boundary virtually coincides with G_w. When there are waves, the surface G_w, deforming, will not be broken up to the moment of destruction of the waves, since in this region there is no turbulence, that is, the wave movement is laminar [2, 3, 9]; in addition, with depth it is self-similar. Accordingly, G_w, the same as G_0, is the surface of a current (we recall that G_w is at a very short distance from G_0).

At the moment $t_0 = 0$ we select an arbitrary small element of the surface $S(t_0)$, outlined by the closed curve $l(\xi, \zeta)$. We will project $l(\xi, \zeta)$ onto the lower boundary G_w of the layer h. Then a small cylindrical element with the volume $V = h(t_0)S(t_0)$ will be cut in the layer h. This volume can be regarded as an analog of a Lagrange particle moving due to the waves, deforming with time in dependence on the wave phase at the particular point but retaining its volume. The condition of conservation of volume follows from the fact that G_w was selected so as to coincide with the surface of the flow and the compressibility of the fluid is neglected. After the time interval dt the element of the wave surface, as a result of the fact that different points on the curve $l(\xi, \zeta)$ move with different velocities, receives the increment $dS(\xi, \zeta)$. Then the relative change (dilatation of a unit surface) during the differentially small time interval dt is

$$dR = dS(l)/S(l), \tag{2.1}$$

and the relative deformation of a surface sector with time is expressed as

$$R(S) = \int S^{-1}(l)\,dS(l) = \ln \frac{S(l)}{C}. \tag{2.2}$$

We will select $t_0 = 0$ in such a way that the dilatation of a surface element, bounded by the $l(\xi, \zeta)$ curve, is equal to zero. Then from (2.2) we have

$$R(S) = \ln [S(l)/S_0(l)], \tag{2.3}$$

or

$$S = S_0 \exp R(S). \tag{2.4}$$

Multiplying both sides of (2.4) by h_0 and taking into account that the volume of the cylindrical element (quasi-Lagrange particle) is conserved during deformations, we obtain

$$h(S)=h_0(S)\exp[-R(S)], \tag{2.5}$$

where h_0 is the thickness of the layer when $t_0 = 0$.

The heat flow through an element of the wave surface $S(\xi, \zeta)$, in accordance with (1.1), is expressed as follows

$$Q=-\int_{(s)} \varkappa \partial_n T\, dS. \tag{2.6}$$

Since the temperature change outside the WF attenuates exponentially, the temperature jump within the limits of the warm film is equal to the temperature difference $\Delta T = T_0 - T_w$ in the h layer. In addition, ΔT and $h \approx \delta$ are related to one another through the Rayleigh boundary number

$$\Delta T=\varkappa\nu(g\alpha)^{-1}\,\mathrm{Ra}\,h^{-3}, \tag{2.7}$$

where g is the acceleration of gravity; α is the coefficient of volume thermal expansion of the water; ν is the kinematic viscosity coefficient. [It was demonstrated in [7] that for the WL Ra = 64.]

Since relationship (2) is used, the results of this point are correct in the case of physical processes near the water-air discontinuity for which this relationship holds true. Despite the fact that the physics of the phenomenon is not explicitly considered, implicitly it is taken into account through the relationship (2.7).

From (2.7) with a sufficient degree of accuracy we have

$$\partial_n T\approx\Delta T/h=(\varkappa\nu/g\alpha)\,\mathrm{Ra}\,h^{-4}. \tag{2.8}$$

Substituting (2.8) into (2.6) and taking (2.5) into account, we obtain

$$Q=-\frac{\varkappa^2\nu}{g\alpha}\mathrm{Ra}\int_{(s)} h^{-4}\,dS=-\frac{\varkappa^2\nu}{g\alpha}\mathrm{Ra}\,h_0^{-4}\int_{(s)}\exp[4R(S)]\,dS. \tag{2.9}$$

In the absence of waves R(S) = 0 and (2.9) gives

$$Q_0=-\frac{\varkappa^2\nu}{g\alpha}\mathrm{Ra}\,h_0^{-4}S_0. \tag{2.10}$$

Accordingly, the coefficient of increase of heat exchange, expressing the ratio of the heat flows when waves are present and absent, has the form

$$N_q=\frac{Q}{Q_0}=\left[\int_{(s)}\exp[-R(s)]\,ds\right]^{-1}\int_{(s)}\exp[4R(S)]\,dS, \tag{2.11}$$

where use was made of the condition of conservation of volume

$$h_0 S_0 = \int_{(S)} h\, dS.$$

Formula (2.11) expresses the ratio of the heat flows in the case of three-dimensional surface waves. For plane waves it is conserved, but in all the relationships derived above S has the sense of the length of the surface wave profile.

Now we will examine specific examples for plane waves. The length of the curve representing the profile of the surface wave in the interval [0, x] of the system, related to the undisturbed surface of the waves, is expressed as follows

$$S = \frac{1}{x}\int_0^x \sqrt{1+(\partial_x \eta)^2}\, dx, \tag{2.12}$$

where η is the equation for the curve forming the wave profile.

Then from (2.12), (2.3), (2.11) for N_q in the case of plane waves we obtain

$$N_q = \left[\int_0^\lambda \left\{\frac{x}{\int_0^x \sqrt{1+(\partial_x \eta)^2}\, dx}\right\}^4 dl\right]^{-1} \int_0^\lambda \left[\frac{1}{x}\int_0^x \sqrt{1+(\partial_x \eta)^2}\, dx\right] dl, \tag{2.13}$$

where λ is wavelength.

Adhering to Monin [10], we will regard S as a function of the mean square wave steepness K, determined in the following way:

$$K^2 = \frac{1}{\lambda}\int_0^\lambda (\partial_x \eta)^2\, dx. \tag{2.14}$$

We will compute the N_q values as a function of K for three models:

1) sinusoidal waves with the profile

$$\eta = a\cos kx, \tag{2.15}$$

2) trochoidal waves, whose profile is stipulated parametrically

$$\chi = (2\pi)^{-1} l\xi + a\sin\xi, \quad \eta = a\cos\xi, \tag{2.16}$$

3) capillary waves with the profile

$$\eta = a\cos kx - \frac{1}{2}a^2 k\cos kx - \frac{1}{12}a^3 k^3 \cos 3kx. \tag{2.17}$$

Figure 2 gives the results of computations of N_q, made using formulas (2.3) -(2.5), (2.7), (2.11)-(2.14), for the models (2.15)-(2.17). Integration was carried out in an interval equal to the wavelength, that is, in phase

from zero to 2π. As a comparison, Fig. 2 also shows the results taken from [10], identical in our case to the value $\exp[R(\lambda)]$. It can be seen that N_q is dependent on wave steepness and increases appreciably with an increase in K. Computations show that with one and the same wave parameters allowance for the existence of a warm film on the ocean surface gives a considerably greater increase in heat flow through the discontinuity, caused by waves, in comparison with that which is determined only by an increase in the mean sea surface due to waves. Since with the very same wave steepness, if a WF is absent, the heat flow due to waves increases by 7-10%; with the existence of a film the increase in the flow is already 50-70%. Despite the fact that with one and the same K a sinusoidal wave gives a greater effect than capillary waves, the latter are stable with considerably greater K values and their total contribution is not less important.

On the basis of the relationships derived above it is possible to analyze the change in the thickness of the warm film and the temperature along the wave. The latter is particularly interesting because there are experiments [14] indicating that the temperature variations ($\Delta\tilde{T}$) along the wave surface are on the order of magnitude of hundredths of a degree ($\Delta\tilde{T}\sim 0$ (10^{-2} °C). A theoretical evaluation of this phenomenon was given in [15]. However, the theory gives results which are considerably too low in comparison with experimental data.

Using formulas (2.5), (2.7), (2.14), (2.15)-(2.17) h and ΔT were computed as functions of the wave phase. The results for sinusoidal and capillary waves are given in Fig. 3, where the change in h and ΔT relative to h_0 and ΔT_0, that is, when waves are absent, is given in percent. It can be seen that the change in h and ΔT along the wave is dependent on K. For example, for K = 0.2, the temperature variations along the wave $(\Delta T) \equiv [(\Delta T)_{max} - (\Delta T)_{min}] = 0(1\%)$ for K = 0.3 accordingly $(\Delta\tilde{T}) = 0(1.5\%)$. If the temperature difference ΔT in the WF is 0(1°), then $(\Delta\tilde{T}) = 0(10^{-2}$ °C). Thus, a result is obtained which is comparable with the experimental data. The change in the thickness of the warm film along a wave is such that for a sinusoidal wave the regions of minimum δ values fall in the neighborhood of the wave phase equal to $\varphi = \pi/4, 5\pi/4$. The maximum δ values are found with $\varphi = 3\pi/4, 7\pi/4$, and the maximum heat flow through the discontinuity exists with $\varphi = \pi/4, 5\pi/4$; the minimum exists with $\varphi = 3\pi/4, 7\pi/4$.

The computations (Fig. 3) show the presence of a phase shift between the wave and the temperature of the surface. Accordingly, there can be nonzero correlations between temperature fluctuations and the vertical component of the wave field. This should lead to the appearance of wave transfer of heat vertically, $Q_\eta = \overline{\tilde{\omega}\tilde{T}}$, in the surface layer of the ocean. Now we will examine this problem in greater detail.

3. Since in the region G_{lam}, lying below the WF and directly adjacent to it, the movement has a quasilaminar character, the excess heat flow through the WF, which appears under the influence of the waves, probably cannot be ensured by turbulent transfer in the region G_{lam}. Accordingly, some other

mechanism must arise here. We will demonstrate that the wave flow, caused by the existence of non-zero correlations between the velocity field, fluctuating with the frequency of waves, and the fluctuations of the temperature field caused by them, can play the role of such a mechanism. Since the phase shift between the wave components of the velocity field and the temperature fluctuations is caused by vorticity and the final rate of heat diffusion, this mechanism must be the most important within the limits of the viscous boundary sublayer adjacent to the ocean surface, that is, where turbulent transfer is still poorly developed.

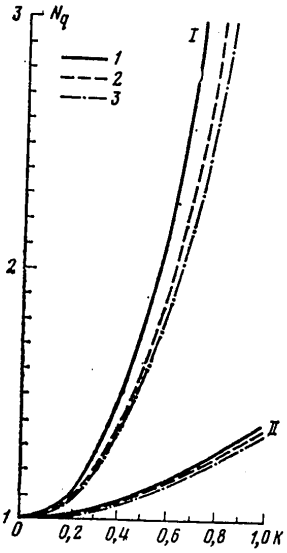

Fig. 2

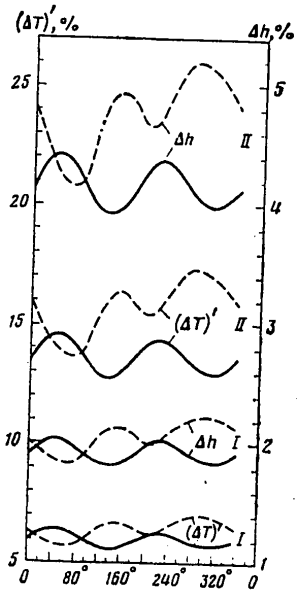

Fig. 3

Fig. 2 (left). Dependence of the coefficient of heat exchange N_q between the atmosphere and the ocean on wave steepness K for sinusoidal (1), trochoidal (2) and capillary (3) waves: I -- taking into account the increase in the surface area of the sea due to waves and the presence of the WF, II -- without allowance for the WF.

Fig. 3. Change in thickness of the warm film Δh and temperature along the wave for the same waves as in Fig. 2.

We will stipulate the ocean surface in a Cartesian coordinate system in the form of one Fourier component of the wave field

$$\zeta = a\cos(kx-\omega t), \tag{3.1}$$

where a is amplitude; k is wave number; ω is wave frequency; t is time; x is the horizontal coordinate. As the characteristic scales we select time ω^{-1}, space independent variables k^{-1}, wave field velocities ($a\omega$). In a curvilinear orthogonal coordinate system

$$\xi = x-\varepsilon\exp(-z)\sin x, \quad \eta = z-\varepsilon\exp(-z)\cos x, \tag{3.2}$$

related to the surface and moving with the wave in which the ξ coordinate coincides with the isolines of the stream function and η is directed within the fluid the equations for the transfer of vorticity Ω and heat have the form

$$[\partial_t + J^{-1}(u\partial_\xi + w\partial_\eta)]\{\Omega, T\} = {}^1/_2\alpha^2\Delta\{\Omega, P^{-1}T\}. \tag{3.3}$$

Here

$$\Omega = J(\partial_\eta u - \partial_\xi w), \quad \Delta = J(\partial_{\xi\xi}+\partial_{\eta\eta}),$$

$$\alpha = (2\nu k^2/\omega)^{1/2} < 1, \quad \varepsilon = ak < 1, \tag{3.4}$$

$\{u, w\}$ are the tangential and normal components of the velocity vector; T are the temperature fluctuations caused by the waves; P is the Prandtl number,

$$J = \partial(\xi, \eta)/\partial(x, z) = J_0 + \varepsilon J_1 + \ldots \tag{3.5}$$

is the Jacobian of the transform such that

$$J_0 = 1, \quad J_1 = -2\exp(-\eta)\cos\xi. \tag{3.6}$$

The boundary conditions at the surface are the conditions of absence of shearing stress

$$w(\xi, \eta=0) = 0. \tag{3.7}$$

and the velocity component normal to ζ

$$\tau_\xi(\xi, \eta=0) \equiv {}^1/_2\alpha^2[\partial_\eta(J^{-1}u) + \partial_\xi(J^{-1}w)]_{\eta=0} = 0 \tag{3.8}$$

For temperature the boundary conditions in accordance with the results in section 2 and in [14, 15] -- there is a phase shift between fluctuations of the surface and the temperature at it -- are stipulated as

$$T(\xi, \eta=0) = T_0\cos(\xi+\gamma), \tag{3.9}$$

where γ is an arbitrary phase shift between ζ and T.

Outside the surface boundary layer for Ω and T we require the attenuation conditions

$$\Omega(\xi,\ \eta\to\infty)=T(\xi,\ \eta\to\infty)=0. \tag{3.10}$$

Solution of the problem (3.3)-(3.10) is sought in the form of a series for the small nonlinearity parameter ε

$$\{\Omega, T, u, w\}=\sum_{m=1}^{\infty}\varepsilon^m\{\Omega_m, T_m, u_m, \varepsilon w_m\} \tag{3.11}$$

with subsequent use of the method of asymptotic "spliced" expansions [16].

We will represent the dynamic characteristics in the form of the sum of values with nonviscous movement and perturbations introduced due to viscosity. Then the dimensionless stream function and velocity have the form $\Psi = -\eta + (\Psi)$, $u = u_0 + (u)$, $w = w_0 + (w)$, where the notations in the parentheses are the viscous perturbations of the Stokes solution, and $u = J^{1/2}\partial_\eta\Psi$. In this case $\Omega_0 = 0$.

In the first approximation for ε we have

$$(\partial_t+u_0\partial_\xi)\{\Omega_1,\ T_1\}={}^1/_2\alpha^2(\partial_{\xi\xi}+\partial_{\eta\eta})\{\Omega_1,\ P^{-1}T\}. \tag{3.12}$$

Taking into account that $u_0 = -1$, $J_0 = 1$ and in our coordinate system $\partial_t \equiv 0$, we rewrite (3.12) in the form

$$[\partial_\xi+{}^1/_2\alpha^2(\partial_{\xi\xi}+\partial_{\eta\eta})]\{\Omega_1,\ P^{-1}T_1\}=0. \tag{3.13}$$

The boundary conditions with $\eta = 0$ are obtained from (3.7)-(3.9) by the substitution of (3.11) in them and equating the corresponding coefficients to zero. In the first approximation

$$\Omega_1(\xi,\ \eta=0)=-2\partial_\xi w_1-2J_1\partial_\xi w_0-u_0\partial_\eta J_1+w_0\partial_\xi J_1, \tag{3.14}$$

$$w_1(\xi,\ \eta=0)=0,\quad T_1(\xi,\ \eta=0)=T_0\cos(\xi+\gamma). \tag{3.15}$$

With $\eta\to\infty$ from (3.10) we have

$$\Omega_1(\xi,\ \eta\to\infty)=T_1(\xi,\ \eta\to\infty)=0. \tag{3.16}$$

In accordance with the asymptotic "spliced" expansions method, the solutions of problems (3.13)-(3.16) are represented as

$$\partial_\xi\{\Omega_{10},\ T_{10}\}=0, \tag{3.17}$$

Then in the approximation (10) the external field equations have the form

$$\Phi_m=\sum_{n=0}^{\infty}\alpha^n\Phi_{mn}. \tag{3.18}$$

whose solutions are

$$\{\Omega_{10},\ T_{10}\}=\{C_{10}(\eta),\ D_{10}(\eta)\}. \tag{3.19}$$

The boundary conditions for (3.19), obtained from (3.16), (3.17), give $C_{10}(\eta) = D_{10}(\eta) = 0$. Thus,

$$\Omega_{10}(\xi, \eta) = T_{10}(\xi, \eta) = 0. \tag{3.20}$$

In the internal field (the boundary layer adjacent to the surface $\eta = 0$) the variables are transformed as

$$\Phi = \Phi^*, \quad r = \eta/\alpha. \tag{3.21}$$

Substituting (3.17) and (3.21) into (3.3), (3.14), in the first approximation for the boundary layer we obtain the equations

$$-\partial_\xi\{\Omega_{10}^*, T_{10}^*\} = {}^1/_2\partial_{rr}\{\Omega_{10}^*, P^{-1}T_{10}^*\} \tag{3.22}$$

with the conditions

$$\{\Omega_{10}^*, T_{10}^*\}_{r=0} = \{-2\cos\xi, \cos(\xi+\gamma)\}. \tag{3.23}$$

The solutions of problems (2.22), (2.23), satisfying the "splicing" conditions with solutions of the external field (3.20), are

$$\{\Omega_{10}^*, T_{10}^*\} = -2\exp(-\eta/\alpha)\{\cos(\xi+\eta/\alpha), \cos(\xi+\eta/\alpha\sqrt{P}+\gamma)\}. \tag{3.24}$$

From (3.24), with an accuracy to the function of ξ, it is possible to determine the horizontal velocity component in the boundary layer, and then from the continuity equation and conditions (3.8), the vertical component. They have the form

$$u_{11} = \sqrt{2}\exp[-\eta/\alpha]\sin(\xi+\eta/\alpha-\pi/4)+F(\xi), \tag{3.25}$$

$$w_{12} = \cos\xi - \exp(-\eta/\alpha)\cos(\xi+\eta/\alpha) - dF(\xi)/d\xi. \tag{3.26}$$

[Velocity $O(\varepsilon\alpha)$ is determined through Ω_{10}.]

Requiring the conditions of limitations on velocity outside the boundary layer, we assume $F(\xi) = 0$. We obtain the velocities of wave movement and temperature to the approximation of ε inclusive

$$\tilde{u} = -1+\varepsilon\exp(-\eta)\cos\xi+\alpha\varepsilon\sqrt{2}\exp(-\eta/\alpha)\sin(\xi+\eta/\alpha-\pi/4), \tag{3.27}$$

$$\tilde{w} = \varepsilon\alpha^2[\cos\xi - \exp(-\eta/\alpha)\sin(\xi+\eta/\alpha-\pi/4)], \tag{3.28}$$

$$\tilde{T} = -\varepsilon 2\exp(-\eta/\alpha\sqrt{P})\cos(\xi+\eta/\alpha\sqrt{P}+\gamma). \tag{3.29}$$

The averaged heat transfer due to waves $\vec{\tilde{Q}}$, $\tilde{Q}\uparrow$ along ξ and η is equal respectively to

$$\vec{\tilde{Q}} = \frac{1}{2\pi}\int_{\xi}^{\xi+2\pi}(\tilde{T}\tilde{u}, \tilde{T}\tilde{w})\,d\xi. \tag{3.30}$$

[In order to obtain a dimensional heat flow it is necessary that $\widetilde{\vec{Q}}\uparrow$ be multiplied by $(\rho \alpha \omega T_0)$, where ρ is water density.]

Substituting (3.27)-(3.29) into (3.30) and carrying out integration, we obtain

$$\vec{\tilde{Q}} = -\varepsilon^2 \left\{ e^{-(1+1/\alpha\sqrt{P})\eta} \cos(\eta/\alpha\sqrt{P}+\gamma) - \right. \\ \left. -\sqrt{2}\, e^{-(1+1/\sqrt{P})\eta/\alpha} \sin\left[\left(\frac{1}{\sqrt{P}}-1\right)\eta/\alpha+\left(\gamma+\frac{\pi}{4}\right)\right]\right\}, \tag{3.31}$$

$$\tilde{Q}\uparrow = \varepsilon^2\alpha^2\{e^{-(1+1/\sqrt{P})\eta/\alpha}\cos[(1/\sqrt{P}-1)\eta/\alpha+\gamma] - \\ -e^{-\eta/\alpha\sqrt{P}}\cos(\eta/\alpha\sqrt{P}+\gamma)\}, \tag{3.32}$$

from which it follows that the heat flow caused by waves is dependent on the phase shift between the surface "rise" and the temperature fluctuations at the surface. Integrating (3.31) for η from zero to infinity, we obtain the integral heat transfer by waves along the horizontal

$$\langle \vec{\tilde{Q}} \rangle = \frac{\varepsilon^2\alpha\sqrt{P}}{2(1+P)}\{(1-P)\cos\gamma+[(1+\sqrt{P})^2-\alpha(1+P)\sqrt{P}]\sin\gamma\} \tag{3.33}$$

It can be seen that in dependence on the phase shift between the "rise" and temperature fluctuations along the wave the integral heat transfer can be in the direction of wave propagation or opposite it.

The role of the mechanism of vertical heat transfer, as follows from (3.32), increases with increasing distance from the free surface, where $\widetilde{Q}\uparrow = 0$; then $\widetilde{Q}\uparrow$ again exponentially decreases.

Thus, as a result of waves there is an increase in the diffusional heat flow through the warm film; this heat flow in the layer lying below the WF and adjacent to it is maintained due to the arising heat transfer mechanism. Below this layer the transfer must be ensured by means of turbulent diffusion. Finally, where the turbulent diffusion mechanism disappears the role of wave transfer must again increase, but in this case it will be caused by internal waves.

It follows from (3.32) that if the lower water layers are warmer, so that the heat flow is directed toward the ocean surface, the temperature field at the surface has a phase shift relative to ζ, belonging to a definite interval of γ changes. However, if the lower layers are cold, that is, $\widetilde{Q}\uparrow > 0$, the phase shift between T in the warm film and the wave must lie in another interval. This is manifested more clearly if (3.32) is expanded into a Taylor series in the neighborhood of the lower boundary of the WF and it is taken into account that dimensionless $\delta \ll 1$. In this case

$$\tilde{Q}(\delta)\uparrow = (\varepsilon^2\alpha/P^{1/2})\delta[\cos\gamma+\sin\gamma], \tag{3.34}$$

hence for $\tilde{Q}(\delta)\uparrow > 0$ and $\tilde{Q}(\delta)\uparrow < 0$ the γ values accordingly belong to different intervals. We note that the effect of a change in the phase shift between the wave fluctuations of temperature along the WF and the rise of the discontinuity in dependence on the sign on $\tilde{Q}\uparrow$ is indicated in experiments which were cited in [15], but there is a need for additional investigations.

Now we will estimate the possible $\tilde{Q}\uparrow$ value. Selecting the parameters of waves equal to a = 50 cm, ω = 1 sec^{-1}, $T_0 = 10^{-1}$ °C, ρ = 1 $g \cdot cm^{-3}$, α = 0.1, ε = 0.1 and substituting them into (3.32), we obtain $\tilde{Q}\uparrow \sim 50$ $cal \cdot day^{-1} \cdot cm^{-2}$. With $T_0 = 5 \cdot 10^{-2}$ °C, α = 0.2, ε = 0.1, $\tilde{Q}\uparrow \sim 100$ $cal \cdot day^{-1} \cdot cm^{-2}$. Thus, the wave flow can compensate the change in the diffusional transfer of heat through the warm film when waves develop.

Figures 4 and 5 show the results of computations of $\tilde{Q}\uparrow$ and $\tilde{Q}_{\downarrow}$ respectively, carried out for some values of the parameters. For all the cited cases P = 7, and ε = 0.1 (since the ε parameter in formulas (3.31), (3.32) enters in the form of a simple factor, with other ε values there is accordingly only a change in the magnitude of the flows). The first and second curves correspond to $\gamma = 10^{-2}$, and the third and fourth -- to γ = 10; for the odd curves -- α = 0.1, whereas for the even curves -- α = 0.3. All the figures give dimensional values of the flows in the units $cal \cdot day^{-1} \cdot cm^{-2}$. In Fig. 4 the curves I, III represent the real values of the flows, whereas curves II and III are reduced by a factor of 10, so that in order to obtain the Q values the corresponding values must be increased by a factor of 10. Figure 5 shows values less than the true values by a factor of 10^3.

It is clear from Fig. 4 that the wave mechanism of "vertical" heat transfer in actuality is important in the intermediate sublayer lying between the warm film and the region with well-developed turbulence. The $\tilde{Q}\uparrow$ value can attain hundreds of calories per day through one square centimeter of horizontal area. Flows of different sign correspond to different phase shifts of thermal wave fluctuations at the ocean surface relative to the surface itself. In this case the flow through the surface itself, where these temperature fluctuations are specifically stipulated, for all γ is equal to zero.

Fig. 5 shows that $\tilde{Q}_{\downarrow}$ is maximum at the surface and then attenuates exponentially, so that in contrast to $\tilde{Q}\uparrow$ for it no double boundary layer is discriminated. The sign on $\tilde{Q}_{\downarrow}$ is also dependent on whether the upper or lower region of the surface layer in the ocean has the higher temperature. As can be seen from a comparison of Figures 4 and 5, in this case the directions of the $\tilde{Q}\uparrow$ and $\tilde{Q}_{\downarrow}$ flows are interrelated.

4. Thus, the presence of a thin temperature boundary layer at the ocean surface should have the result that with the appearance of waves there is an increase in heat diffusion through the atmosphere - ocean discontinuity.

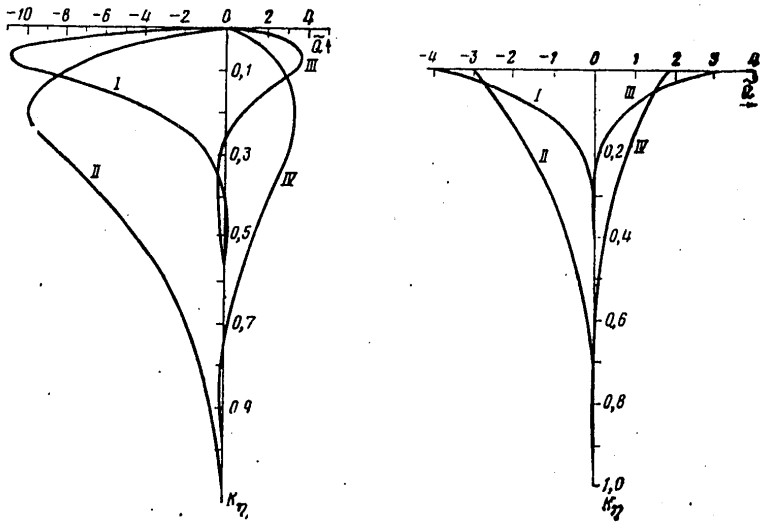

Fig. 4. Distribution of vertical heat flows $\tilde{Q}\uparrow$ caused by waves as a function of η with $\varepsilon = 0.1$, P = 7; I) $\alpha = 0.1$, $\gamma = 10^{-2}$; II) $\alpha = 0.3$, $\gamma = 10^{-2}$; III) $\alpha = 0.1$, $\gamma = 10$; IV) $\alpha = 0.3$, $\gamma = 10$.

Fig. 5. Distribution of horizontal heat flows Q caused by waves as a function of η with the same values of the parameters as in Fig. 4.

An analysis shows that this additional flow can be caused by the wave mechanism of heat transfer vertically in the layer directly adjacent to the warm film. This corr ponds to the experimental data in [12]. The wave flow is a result of the nonpotentiality and nonlinearity of wave motion and attenuates exponentially with increasing depth. In the region of its disappearance the main role must evidently be played by turbulent transfer or the similar wave flow caused by internal waves.

We note in conclusion that the mechanism of wave transfer of heat in a vertical direction was also studied in [17], where the problem was formulated in a Cartesian coordinate system, which makes difficult a sufficiently rigorous analysis of the thin boundary layer directly adjacent to a moving discontinuity; therefore, in this article the problem was considered in a curvilinear coordinate system directly related to wave movement.

The author expresses sincere appreciation to the reviewer for useful comments.

BIBLIOGRAPHY

1. Schooley, A. U., "Temperature Differences Near the Sea-Air Interface," J. MARINE RES., 25, No 1, 1967.

2. Khundzhua, G. G., Andreyev, Ye. G., "Experimental Investigations of Heat Exchange Between the Sea and the Atmosphere in the Case of Small-Scale Interaction," IZV. AN SSSR, FAO (News of the USSR Academy of Sciences, Physics of the Atmosphere and Ocean), 13, No 10, 1977.

3. Khundzhua, G. G., Gusev, A. I., Andreyev, Ye. Ye., Gurov, V. V., Skorokhvatov, N. A., "Structure of the Surface Cold Film of the Ocean and the Atmosphere," IZV. AN SSSR, FAO, 13, No 7, 1977.

4. Hill, R. H., "Laboratory Measurement of Heat Transfer and Thermal Structure Near an Air-Water Interface," J. PHYS. OCEANOGR., 2, No 2, 1972.

5. Ginzburg, A. I., Zatsepin, A. G., Fedorov, K. N., "Fine Structure of the Thermal Boundary Layer in the Water at the Air-Water Discontinuity," IZV. AN SSSR, FAO, 13, No 12, 1977.

6. Katsaros, K., Liu, W. T., Businger, J. A., Tillman, J. E., "Heat Transport and Thermal Structure in the Interfacial Boundary Layer Measured in an Open Tank of Water in Turbulent Free Convection," J. FLUID MECH., 83, Part 2, 1977.

7. Ginzburg, A. I., Fedorov, K. N., "The Rayleigh Critical Boundary Layer With Cooling of Water Through a Free Surface," IZV. AN SSSR, FAO, 14, No 4, 1978.

8. Ginzburg, A. I., Fedorov, K. N., "Thermal State of the Boundary Layer of Cooling Water With Transition from Free to Forced Convection," IZV. AN SSSR, FAO, 14, No 7, 1978.

9. Ball, F. K., "Sea Surface Temperatures," AUSTRAL. J. PHYS., 7, 649-651, 1954.

10. Monin, A. S., "Surface Area of a Wave-Covered Sea," IZV. AN SSSR, FAO, 3, No 6, 1967.

11. Witting, J., "Effects of Plane Progressive Irrotational Waves on Thermal Boundary Layer," J. FLUID MECH., 50, Part 2, 1971.

12. Yefimov, V. V., Zapevalov, A. S., "Spectral Characteristics of Temperature Pulsations in the Wind Waves Layer," OKEANOLOGIYA (Oceanology), 15, No 4, 1975.

13. Grapper, G. D., "An Exact Solution for Progressive Capillary Waves of Arbitrary Amplitude," J. FLUID MECH., 2(6), 532, 1957.

14. Van der Watering, W. P. M., Wiggert, J. C., "Surface Temperature Fluctuations Due to Waves," TRAN. AMER. GEOPHYS. UNION, 49, 204, 1968, Paper Presented at the Spring Meeting of the American Geophys. Union, Washington, D. C., April, 1968.

15. O'Brien, E. E., Omholt, T., "Heat Flux and Temperature Variation at a Wavy Water-Air Interface," JGR, 74, No 13, 1969.

16. Cole, J., METODY VOZMUSHCHENIY V PRIKLADNOY MATEMATIKE (Perturbation Methods in Applied Mathematics), "Mir," 1972.

17. Nelepo, B. A., Dvoryaninov, G. S., Prusov, A. V., "Generation of Stationary Temperature Boundary Layers by Surface Waves," IZV. AN SSSR, FAO, 14, No 1, 1978.

[25-5303]

5303
CSO: 1866

UDC 551.465.41:532.529.2

STRUCTURE OF THERMOCONCENTRATION CONVECTION IN A STRATIFIED FLUID

Moscow IZVESTIYA AKADEMII NAUK SSSR, FIZIKA ATMOSFERY I OKEANA in Russian
Vol 15, No 9, 1979 pp 964-973

[Article by V. A. Popov and Yu. D. Chashechkin, All-Union Scientific Research Institute of Physical-Technical and Radioelectronic Measurements, submitted for publication 20 October 1978]

Abstract: An experimental study was made of the formation of the structure of thermoconcentration convection, periodic vertically, during the propagation of a warm front in a fluid with a stably stratified salinity distribution. For a plane front, the normal to which forms an angle ±19, ±11° to the horizon, the critical value of the Rayleigh number, characterizing the onset of formation of cells is $Ra_{cr} = g\alpha\Delta Th^3/\nu\chi = 3700\pm1000$. For a cylindrical front (heater-vertical filament) $Ra_{cr} = 16\ 000\pm5000$. The formation of the cells also occurs with a local change in the T-, S-characteristics, leading to the formation of salt fingers, outside the zone of the fingers and within it, after the degeneration of "fast" vertical convection. With the formation of cells in this case $5000 < Ra_{cr} < 20\ 000$.

[Text] Interest in laboratory investigations of the structure of convective currents during the heating of a stratified fluid is related to study of the role of double diffusion processes in the formation of the fine structure of the ocean [1]. As a result of these laboratory experiments it was established that with the horizontal propagation of one scalar characteristic (temperature) in a stratified fluid, whose density distribution is ensured by a vertically variable distribution of another impurity (salt), in the case of greatly differing kinetic coefficients (thermal conductivity coefficient χ and diffusion coefficient k_S), there is formation of eddy convective cells which are vertically periodic [2-5].

The formation of convective cells is associated with the following two properties of a stratified fluid, whose density in an undisturbed state varies with height: $\rho = \rho(z)$; the scale of density change is $\Lambda = (d \ln \rho/dz)^{-1}$. As a result of the stratification effect the height of rising of a heated particle of fluid, retaining its initial salinity, is limited due to the hydrostatic stability condition: the density of a floating-up heated particle of fluid must be less than or equal to the density of the fluid at the new level $\rho(T_0+\Delta T, S(z)) \leqslant \rho(T_0, S_0(z+h))$. Due to the great difference in the values of the kinetic coefficients the fluid particles can be rapidly replaced by only one scalar characteristic (heat) with an almost constant value of the other (salt concentration). With the propagation of a warm front in an aqueous solution of common salt ($\chi = 1.43 \cdot 10^{-3}$ cm^2/sec, $k_S = 1.41 \cdot 10^{-5}$ cm^2/sec) a fluid particle receives heat from the heated wall, transports it through the convective cell and carries an undisturbed fluid to the leading edge of the warm front [4, 5] or the cold wall in experiments in a narrow cell [3] virtually without a change in its salinity. The forming convective currents redistribute the initial distribution of salinity vertically -- at the boundaries of the cells the concentration gradient is considerably greater than within. The temperature gradient and velocity shear are also maximum at the boundaries between adjacent cells, separated by thin fluid layers at rest [5].

In a theoretical analysis of the system of equations describing the processes of thermoconcentration convection, it is important to make a choice of the scale length employed for deriving equations in dimensionless form. In a narrow cell as the scale length d we select the cell width [3, 6]; in a study of the thermoconcentration convection in large, broad basins -- the thickness of the heated layer D^* (that is, the distance from the leading edge of the warm front to the heater) [3, 5] or in our notations, the scale h [4, 5, 7] by which the density of a heated element, floating up with the retention of its salinity, becomes equal to the density of the undisturbed stratified fluid $\rho(T_0+\Delta T, S(z_0)) = \rho(T_0 S(z_0+h))$, $h = \alpha \Delta T \Lambda$. Here α is the coefficient of thermal expansion of the fluid, ΔT is the heating temperature, T_0 is temperature of the fluid, S(z) is salinity. With such a choice of the scale length in the dimensionless equations of motion and diffusion we will have the Rayleigh thermal number [6] $Ra_T = g\alpha \Delta T d^3/\nu\chi$, the Rayleigh saline number [6] $Ra_S = gd^4/\nu k_S \Lambda$, the Rayleigh number $Ra = g\alpha \Delta T n^3/\nu\chi$ (g is the acceleration of gravity), determining the current regimes [4, 5, 7].

Experimental investigations carried out in a broad basin demonstrated that in the propagation of a plane vertical thermal front the vertical dimension of the forming cells is equal to the height of rising of the fluid to the level of neutral buoyancy $h = \alpha \Delta T \Lambda$. The formation of the cells begins when the Rayleigh number exceeds a critical value equal to Ra = 15 000±2500 [4] and Ra = 4500±1000 [5]; the Rayleigh thermal and saline numbers, constructed using the thickness of the heated layer D^*, according to the data in [5], satisfy the expression $Ra_T = g\alpha \Delta T D^{*3}/\nu\chi = 0.059\ Ra_S^{5/6} = 0.059\ (gD^{*4}/\nu k_S \Lambda)$, obtained in [3, 6] for a narrow cell with the width

d on the assumption that the horizontal gradient of density is equal to zero.

In the case of a sloping heated wall the critical values of the Rayleigh number $Ra_h = g\alpha\Delta T \cos\vartheta h^3/\nu\chi = Ra \cos\vartheta$ lie in the range $10\,000 < Ra_h < 20\,000$ with $\vartheta < 60°$. The experiments were carried out with $\vartheta = 31.5, 45, 58.5°$; with $\vartheta = 75.8°$ we have $35\,000 < Ra_h < 60\,000$ (see [8]). Here and in the text which follows ϑ is the angle between the normal to the warm front and the horizon (Fig. 1). The experiments [8] were carried out with lateral heating of a water solution of sugar. In the case of large angles of slope, when the heat flow is propagated almost vertically, the nature of formation of the structure of convective currents changes.

With mixing of fluids with close density values but different concentrations of salt and sugar, arriving from several spatially separated sources, due to the difference in the diffusion coefficients of sugar k_S and salt k_S ($k_S:k_S = 1:3$) there can also be formation of layers of fluid with considerable vertical gradients separated by layers of fluid with an almost constant density [9].

The double diffusion processes play a definite role in forming the fine structure of the ocean [1], the structure of distribution of admixtures in decanted fluid [10], the redistribution of the concentration of admixtures in the growing of monocrystals or particles in turbid and suspension-carrying flows, and in the dynamics of heat transfer in a stratified fluid. In this connection it is of interest to investigate the influence of the boundary conditions (direction of propagation and form of the warm front) on the dynamics of formation and type of structure in a stratified fluid (SF).

The experiments were carried out in a basin with a length of 30 cm, a width of 10 cm and a height of 25 cm, filled with a SF with a density gradient constant with depth. Visualization of the structure was accomplished using an IAB-451 shadow instrument with a vertical slit 0.02 x 10 mm in the illuminating part and a flat knife in the receiving part. Temperature fluctuations were measured using a specially developed converter in which use was made of the pulsed sounding method, making it possible to increase response when working in fluids at rest [11]; the sensing element was an MT-54 thermistor. Temperature difference measurements were made using a copper-constantan thermocouple whose hot junction was placed on the heated wall or at a point of interest in the fluid, whereas the cold junction was placed on a lateral wall of the basin. The period of free internal oscillations $T^* = 2\pi(\Lambda/g)^{1/2}$ was determined using the density mark method on the basis of measurement of the period of waves excited by the wake of a vertically floating-up bubble [12]. The method for the experiments and apparatus are described in greater detail in [5]. The experiments were carried out in a fluid with a constant density gradient $\Lambda = 1300$ cm, $T^* = 7.2$ sec, $\Lambda = 2100$ cm, $T^* = 9.2$ sec.

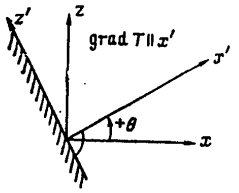

Fig. 1.

Orientation of heater surface.

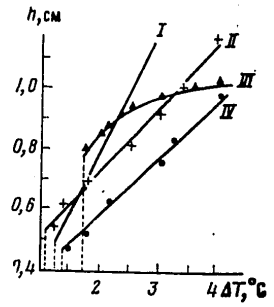

Fig. 2.

Dependence of vertical dimension of convective cell on heating temperature: Λ = 1300 cm, T = 7.2 sec, I -- ϑ = 0, II -- ϑ = -11°, III -- filament, IV -- ϑ = 19°.

Table 1

ϑ, degrees	-19	-11	0	11	19
h_{cr}, cm	0.55	0.53	0.53	0.5	0.48
ΔT_{cr}, °C	1.0	1.12	1.25	1.38	1.46
$Ra_{cr} = g \quad Th^3/$	3500	3600	4000	3500	3400

Investigations of the influence of the heater slope on the dynamics of setting in of a periodic structure were carried out with small slope angles ϑ = ±19, ±11, 0° (in Fig. 1 the positive angle is reckoned clockwise, ϑ = 0° corresponds to a vertically oriented heater). The time constant of the heater at the 0.7 level was 1.5 minutes.

During the propagation of a plane thermal front at an angle to the horizon the general pattern of currents is similar to that observed with ϑ = 0 [5]. Convective cells are formed along the entire surface of the heater with attainment of the critical temperature of heating, whose values are given in Table 1 (Λ = 1300 cm). Figure 2 gives the dependence of the vertical dimension of the cells on the heating temperature (the temperature difference between the heated and opposite cold wall of the basin). At the time of formation the vertical dimension of the forming cells decreases with an increase in the angle of slope ϑ. In this case the critical value of the Rayleigh number, corresponding to the moment of closing of the system of eddies, remains virtually constant because the heating temperature increases with an increase in the angle of slope (see Table 1); $\nu = 10^{-2}$ cm^2/sec, $\chi = 1.43 \cdot 10$ cm^2/sec, $\alpha = 3.06 \cdot 10^{-4}$ grad^{-1}.

If the heater temperature is maintained constant, the vertical dimension of the cells does not change; in the horizontal direction the length of the cell increases proportionally with time until the opposite wall of the basin is reached. If the heating temperature increases, the vertical

dimension of the cells increases (see Fig. 2); for all the investigated angles h = a + bh, where h = $\alpha \Delta T \Lambda$; the a and b values are given in Table 2.

Table 2

γ, degrees	-11	0	19
a, cm	0.29	0	0.185
b	0.55	1	0.49

Table 3

φ, град degrees	ΔT, °C	$h = a\Delta T\Lambda$, см	h_1, см	h_2, см	h_3, см	h_4, см	h_5, см	h_6, см	h_7, см	h_8, см	$h_{ср}$ см mean	σ_h
-11	4	1,59	1,02	1,02	1,2	1,02	1,32	1,45	1,45	1,24	1,18	0,16
0	2,7	1,07	1,2	1,02	1,25	1,07	1,15	0,94	1,11	0,94	1,11	0,11
19	4	1,59	1,81	1,07	1,07	0,94	0,85	1,02	0,98	0,90	0,96	0,10

The dependence of the critical values of heating temperature on heater orientation can be governed by the influence of diffusion currents of the fluid caused by curvature of the lines of constant density near the sloping boundaries [13]. In this case there is formation of an ascending ($\vartheta < 0$) or descending ($\vartheta > 0$) flow; these flows accordingly accelerate or decelerate the thermoconvective current which arises and accordingly increase or decrease the critical height h_{cr} of the thermoconvective cell.

In this case the error in determining the Rayleigh number is determined by the inaccuracy in determining ΔT, h: $\delta(Ra)/Ra = \delta(\Delta T)/\Delta T + 3\delta h/h$. Table 3 gives the vertical dimensions of cells obtained when making photometric measurements of current kinograms with t = 20 min from the moment of activation of the heater in the IFO-451 microphotometer.

The relative error in measuring temperature in these experiments is 3%; then, taking into account the data in Table 3, the error in determining the Rayleigh number is 33%.

The convective axially symmetric periodic structure arising around the heated filament, although it exhibits a considerable external similarity to the plane problem, differs significantly in fine details. In this case the heater was an MGTF-0.07 lead with an external diameter d = 0.8 mm. Figure 3 shows shadow kinograms demonstrating the development of the periodic structure with time after heating is started. The expanding cylindrical warm front, which corresponds to the dark band on the right side and the light

band on the left side of Fig. 3,a creates horizontal temperature gradients $\partial T/\partial x \lesssim 0$. An ascending convective flow begins to be formed near the heater; it transfers to this level a more saline fluid from the lower-lying layers. The velocity maximum is situated at a small distance from the heated filament. A complex density distribution arises within the heated layer -- the density gradient $\partial\rho/\partial r > 0$ at the outer boundary of the warm front. Then its value decreases somewhat as a result of rising of the above-lying fluid, which leads to a corresponding decrease in $\partial n/\partial r$, since in an aqueous solution the refraction coefficient and density are related by the linear expression [14] $n(z) = 1.3330 + 0.231\ [\rho(z) - 1]$, and the corresponding change in the distribution of illumination on the shadow photograph. A decrease in the $\partial\rho/\partial r$ value leads to the formation of a gray band near the heater on the left half of the photograph in Fig. 3,a; near the heater $\partial\rho/\partial r$ again increases.

A further temperature increase leads to the development of current instability and a periodic structure begins to form virtually simultaneously in the entire depth of the fluid. The arising nonuniformities of the refraction coefficient gradient have a complex bell-like configuration (see Fig. 3,b); they are elongated in the upper part near the heater, then deviate somewhat from it (become broader) and at the distance r = 6 mm from the axis drop sharply downward. Formation of the structure is accompanied by the excitation of internal waves of a zero frequency, whose length is equal to the vertical dimension of the cells (see Fig. 3,c, $\Delta T = 1.75°$ C).

A further temperature increase leads to the formation of axially symmetric convective cells in which layers with a small density gradient are separated by thin "sheets" with great gradient values. All the layers are at the angle $\beta = 24°$, $\sigma_\beta = 3.5°$ (each t = 20 min) to the horizon. The boundaries of the layers rise sharply and converge near the filament; their traces can be made out in the extent of several cells. A further temperature increase leads to a decrease in the number of cells and a decrease in their slope to the horizon (Fig. 3,d $\Delta T = 4.0°$C, t = 40 min, $\beta = 10°$, $\sigma_\beta = 2°$). Figure 4 shows the results of photometric measurements of a negative corresponding to the kinogram in Fig. 3,d in the vertical (at a distance r = 1.5 cm from the heater) and horizontal directions. (Here η is the blackening density in arbitrary units; x, z are the distances from the filament and along it.) In the vertical section it is necessary to discriminate sharply expressed thin sheets with high values of the gradient of the refraction coefficient (the ratio of the gradients outside and inside the sheet is (3±1):1, the ratio of the thicknesses of the layer and sheet is (5±1):1) and note the existence of considerable fluctuations of the density gradient within the cell. The boundaries of the layers curve sharply near the filament, but their traces can be followed for a considerable distance; sometimes they rise upward 2-4 cells (see Fig. 3, c, d). On the photogram $\eta(r)$ it is possible to discriminate two zones in the region of the ascending current: a zone of laminar flow adjacent to the filament

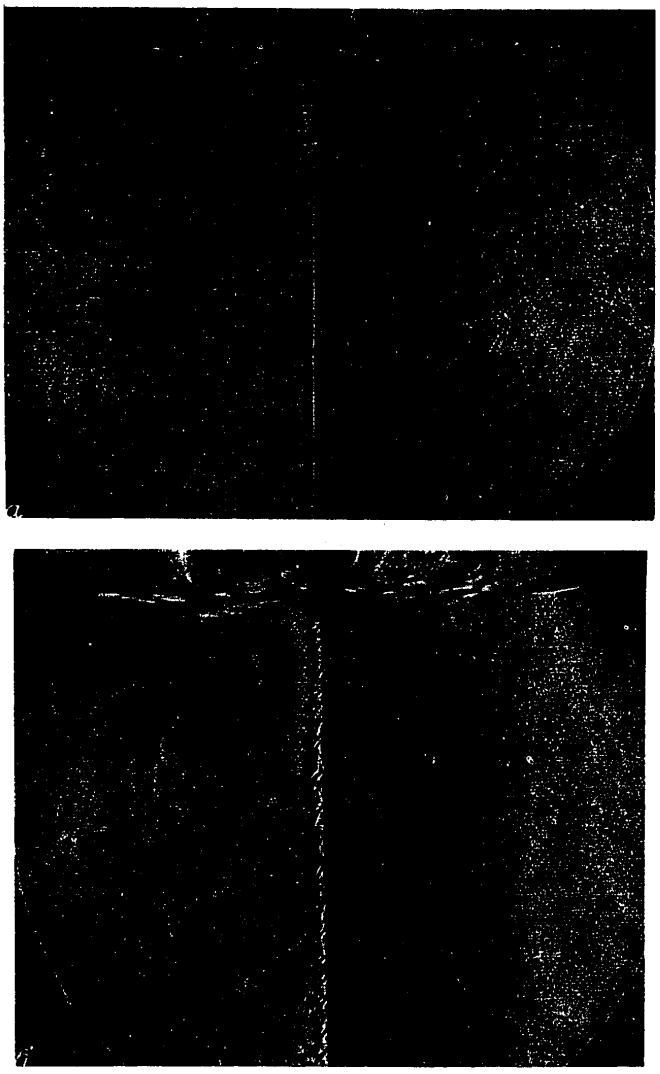

Fig. 3. Shadow photographs of convective current, heater - vertical filament: a -- t = 1 min, b -- t = 2.5 min, c -- t = 20 min, d -- t = 40 min

(from the boundary of the filament to r = 1.2-1.6 mm) and a zone of the velocity maximum in which it is possible to make out the traces of sharp density gradients at the boundaries of the cells, causing considerable fluctuations of blackening density $1.6<r<2.3$ mm, situated between the filament and the regular cells. The density disturbance is considerably greater in the upper part of the cells where it is carried by the deviating convective current than in the lower part, where the fluid from the undisturbed

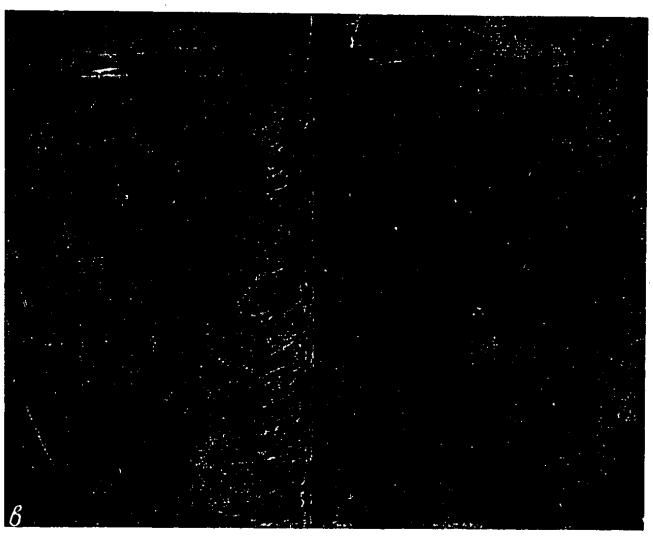

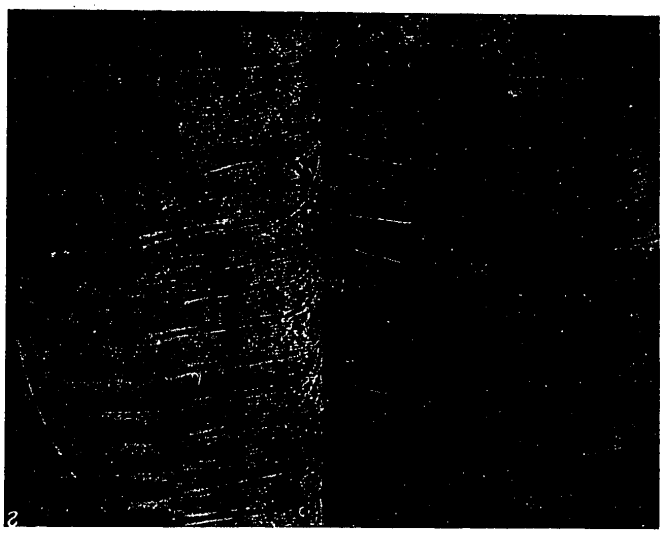

regions flows down. Thereafter, if the heating temperature is not changed, the cells grow in a horizontal direction. If the heating temperature (the temperature difference between the filament and the wall) increases, there

is also an increase in the height of the cells, but in contrast to a plane case $h = 0.95(\alpha\Delta T\Lambda)^{1/2}$. In this case the critical value of the Rayleigh number is substantially greater than for the plane problem: Ra_{cr} = 16 000± 5000, ΔT_{cr} = 1.75°C, Λ = 1300 cm.

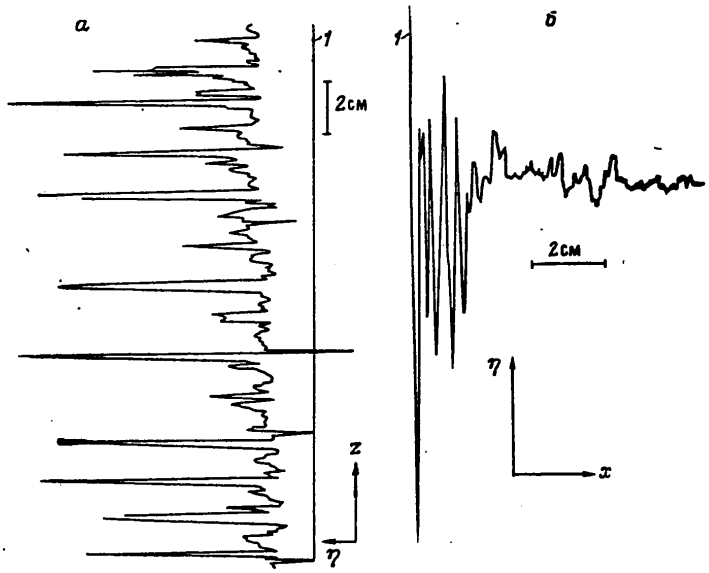

Fig. 4. Dependence of negative blackening density in arbitrary units on distance: a) photometric measurement in vertical direction, b) in horizontal direction, 1) heater - filament.

A layered structure of a homogeneous stratified fluid is also formed if the distribution of the T, S characteristics changes within it in a limited volume, for example, with the introduction of a small volume of heated saline fluid into the near-surface layer or fresh and cold fluid into the bottom layer at a sufficiently small rate ($v<0.1$ cm/sec), that is, when a situation prevails leading to the formation of salt fingers in a limited volume. The general picture of the current coincided for both cases. Figure 5 shows shadow kinograms of the structure arising with the melting of a small piece of ice (basin temperature T_0 = 19°C). Immediately after being introduced an intensive melting of the ice begins; the forming fresh cold water floats up in the form of individual thin streams with a diameter of 0.5-1 mm at the height H = 4-5 cm (freshened "fingers" in salt water). In this case there is formation of a structure of thin alternating cold and warm layers (heat exchanger) and the entire region of relatively rapid

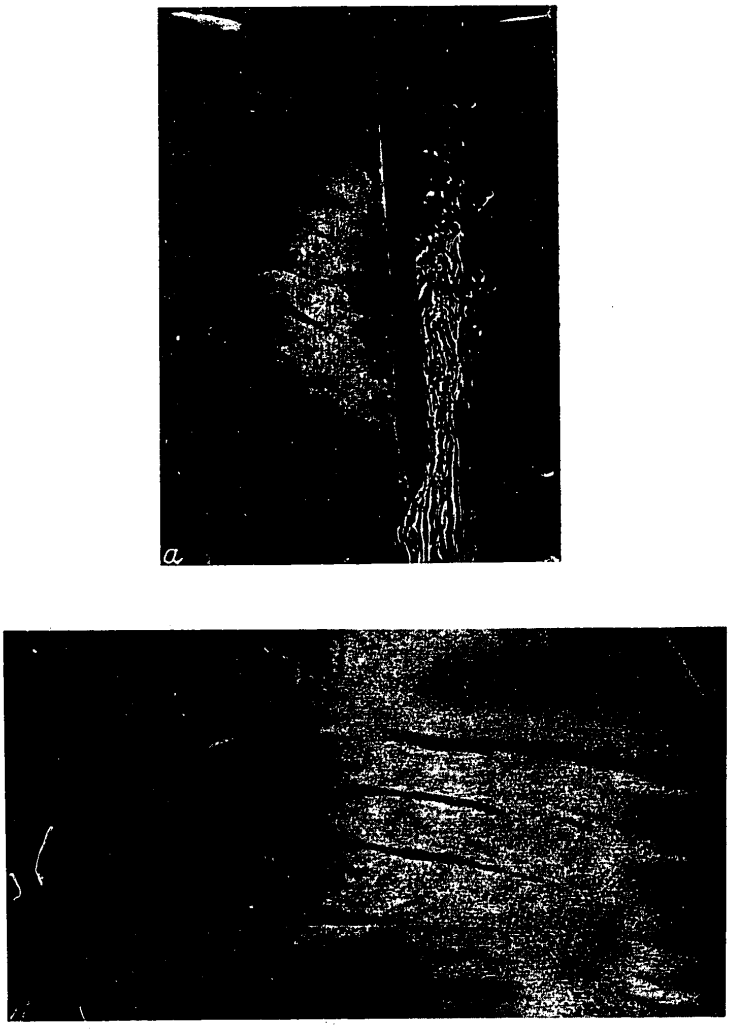

Fig. 5. Shadow photographs of structure of convective current with local disturbance of T,S characteristics of fluid.

vertical "finger" convection is somewhat cooled. Outside it there is propagation of a cold front of a complex form, and the first eddy begins to form near the region of the fingers, in the zone of the maximum horizontal gradients $\partial T/\partial x$, $\partial S/\partial x$ after t = 4 min from the onset of the process (see Fig. 5,a).

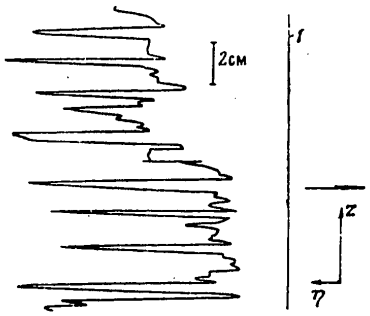

Fig. 6. Change in blackening density of negative (vertical direction) (formation of cells during thawing of ice). 1 -- vertical over melting ice.

The temperature sensor, placed in the zone of "finger" convection, registers marked cooling and a gradual increase in mean temperature, accompanied by gradually attenuating nonstationary oscillations $\langle\Delta T\rangle = 0.05°C$, $\sigma_T = 0.03°C$ with degeneration of finger convection. As a result of general cooling of the zone in the fluid there is maintenance of $\partial T/\partial x$ gradients adequate for continuing formation of the structure. At the same time a cooled wall mechanism is operative on all boundaries of the zone of finger convection and after degeneration of the "fast" heat transfer process. In this case the layers forming in the central part are sloped downward (in the direction of the mean flow of fluid). In microphotometric measurements it is easy to make out individual cells (Fig. 6) and fluctuations of blackening density caused by convective flow within the cells. The total change in negative blackening level is associated with the nonuniformity in vertical temperature distribution. The formation of cells in a fluid with the density scale $\Lambda = 2100$ cm begins with supercooling $\Delta T = 0.9$-$1.0°C$. In this case $h = \alpha\Delta T\Lambda = 0.64$ cm and the observed dimensions of the cells are h = 0.62, 0.7, 0.84, 1.0 cm, which correspond to Rayleigh numbers Ra = 5000, 7000, 12 000, 20 000. Thereafter the dimensions of the cells are somewhat evened out and when t = 20 min we obtain $\Delta T = 1.5°C$, $h = \alpha\Delta T\Lambda = 0.96$ cm, $\langle h\rangle = 1.16$ cm, $\sigma_h = 0.16$ cm. The forming structure advances both outwards from the zone of the fingers and within it as the finger convection degenerates. With joining of the cells the Rayleigh number attains a maximum; then it decreases and accordingly there is a degeneration of the convective current within the cells. But within the fluid for a long time (4-5 hours) there is retention of a zone of increased and decreased values of the salinity gradient; there are traces of the boundaries of cells which are slowly destroyed by molecular diffusion processes. The height of the convection zone is determined by the verical dimension of the "finger convection" region and is dependent on the total difference in densities and temperatures of the introduced fluid and the fluid at rest, whereas the

horizontal dimensions are dependent on the difference in the heat content of the fluids.

Our experiments indicated that a periodic convective structure arises with the propagation of a warm front of an arbitrary shape if the arising temperature differences at the defined horizon exceed a critical value. In this case for a solution of common salt $\Delta T = 1\text{-}2°C$ the formation of a structure occurs with Rayleigh numbers $Ra_{cr} = 5000\text{-}20\,000$, which coincides with evaluations of the critical number $10^4 < Ra_{cr} < 2 \cdot 10^4$, cited in [7] using the results of numerical computations of current stability with activation of heating of the lateral wall in a wide cell. The height of the cells is determined by the degree of heating and the initial stratification of the fluid $h_s = a + bh$, $a = 0$, $b = 1$ with $S = 0$, $h = \alpha \Delta T \Lambda$ in a plane problem and $h = 0.95(\alpha \Delta T \Lambda)^{1/2}$ for an axially symmetric problem. The principal reason for formation of cells is lateral diffusional instability, since during the propagation of a warm front a horizontal temperature gradient $\partial T / \partial x < 0$ arises in the stratified fluid, a horizontal salinity gradient $\partial S / \partial x \neq 0$ and a horizontal density gradient $\partial \rho / \partial x > 0$ ("input" and "output" in the equation for vorticity cited in [3]).

BIBLIOGRAPHY

1. Fedorov, K. N., TONKAYA TERMOKHALINNAYA STRUKTURA VOD OKEANA (Fine Thermohaline Structure of Ocean Waters), Gidrometeoizdat, 1976.

2. Gubin, V. Ye., Khaziyev, N. N., "Thermoconcentration Convection," IZV. AN SSSR, MEKHANIKA ZHIDKOSTI I GAZA (News of the USSR Academy of Sciences, Mechanics of Fluid and Gas), No 3, 166-169, 1970.

3. Thorpe, J. A., Hutt, P. K., Soulsby, R., "The Effect of Horizontal Gradients on Thermohaline Convection," J. FLUID MECH., 38, No 3, 375-400, 1969.

4. Chen, C. F., Briggs, D. G., Wirts, R. A., "Stability of Thermal Convection in a Salinity Gradient Due to Lateral Heating," INT. J. HEAT. MASS TRANSFER, 14, No 1, 57-66, 1971.

5. Nekrasov, V. N., Popov, V. A., Chashechkin, Yu. D., "Formation of a Periodic Structure of Convective Flow With Lateral Heating of a Stratified Fluid," IZV. AN SSSR, FAO (News of the USSR Academy of Sciences, Physics of the Atmosphere and Ocean), 12, No 11, 1191-1200, 1976.

6. Hart, J. E., "On Sideways Diffusive Instability," J. FLUID MECH., 49, No 2, 279-288, 1971.

7. Chen, C. F., "Onset of Cellular Convection in a Salinity Gradient Due to a Lateral Temperature Gradient," J. FLUID. MECH., 63, No 3, 563-576, 1974.

8. Chen, C. F., Paliwal, R. C., Wong, S. B., "Cellular Convection in a Density Stratified Fluid: Effect of Inclination of the Heated Wall," PROC. HEAT TRANSFER FLUID MECH. INST., Davis, Calif., 18-32, 1976.

9. Turner, J. S., Chen, C. F., "Two-Dimensional Effects in Double-Diffusive Convection," J. FLUID MECH., 63, No 3, 577-592, 1974.

10. Zavgorodnyy, G. F., Kolesnik, V. I., Povkh, I. L., Sevost'yanov, G. M., "Concentration Convection in a Hardening Melt," PMTF (Applied Mechanics and Technical Physics), No 6, 98-103, 1975.

11. Levtsov, V. I., Chashechkin, Yu. D., "Measurement of the Conductivity of a Fluid by the Pulsed Sounding Method," TEZISY DOKLADOV III VSESOYUZN. SEMINARA-SOVESHCHANIYA "METROLOGIYA V RADIOELEKTRONIKE" (Summaries of Reports at the Third All-Union Seminar-Conference "Metrology in Radioelectronics"), VNIIFTRI, 188-189, 1975.

12. Nekrasov, V. N., Chashechkin, Yu. D., "Measurement of the Velocity of Currents and the Period of Internal Oscillations of a Fluid by the Density Marks Method," METROLOGIYA (Metrology), No 11, 19-23, 1974.

13. Phillips, O. M., "On Flows Induced by Diffusion in a Stably Stratified Fluid," DEEP SEA RES., 17, 435-443, 1970.

14. Mowbray, D. E., "The Use of Schlieren and Shadowgraph Techniques in the Study of Flow Patterns in Density Stratified Liquids," J. FLUID MECH., 27, No 3, 595-608, 1967.

[25-5303]

5303
CSO: 1866

UDC 551.465.41

INVESTIGATION OF THE FINE VERTICAL STRUCTURE OF WATER DENSITY IN THE OCEAN BY THE OPTICAL INTERFERENCE METHOD

Moscow IZVESTIYA AKADEMII NAUK SSSR, FIZIKA ATMOSFERY I OKEANA in Russian
Vol 15, No 8, 1979 pp 855-863

[Article by V. S. Belyayev, V. L. Vlasov and R. V. Ozmidov, Institute of Oceanology, submitted for publication 22 August 1978]

Abstract: The authors describe a method for measuring the fine structure of the density field in the ocean in situ using a laser photoelectric interferometer. Measurements in the upper thermocline revealed layers with a thickness about 1 m, within which there are density inversions with vertical scales of 5-10 cm. The spectra of fine structure of the density field in the range of scales from 1 to 8 m are well approximated by a power-law dependence with an exponent close to -3. The nature of the change in the coherence of density fluctuations for time shifts from 0.5 to 2 hours is different for fluctuations with vertical scales less than and greater than 8 m. The possibility of an influence of internal waves on the temporal variability of fine structure of the density field with vertical scales greater than 8 m is noted.

[Text] The fine vertical structure of the water density field ρ in the ocean is at present determined in situ by indirect methods by simultaneous measurement of the distribution of water salinity S, its temperature T and hydrostatic pressure p. Salinity is also usually determined indirectly using the conductivity of water C, which is dependent on T, S and p, and also on the chemical composition of salts (for example, see [1]). The ρ, T, S, p and C values are related to one another by complex, generally speaking, nonlinear dependences; therefore for determining ρ from measured T, S and p (or T, C and p) use is made of the empirical formulas of state of sea water or special oceanological tables [2]. The results obtained in this case contain

definite systematic errors [3, 4]. However, the equations of state of sea water are constantly being refined [4] and at the present time a high accuracy in determining the conductivity of sea water in principle makes it possible (with a corresponding accuracy in measuring temperature and pressure) to compute density ρ with an error of $\pm 2 \cdot 10^{-6}$ g·cm^{-3}. But errors in determining ρ can also be introduced due to variations in the isotopic composition of water and salts (error up to $\pm(3\text{–}7) \cdot 10^{-6}$ g·cm^{-3}), and also as a result of the different quantity of gases dissolved in the water ($\pm 1.5 \cdot 10^{-6}$ g·cm^{-3}).

In indirect methods for determining ρ in situ the error usually increases due to the inaccuracy in determining T, S, p and C. In standard sounding apparatus the accuracy in determining T usually does not exceed 0.02°C, salinity (on the basis of conductivity) — 0.02°/oo, pressure -- 0.1% of the measured value, which leads to an error in determining ρ up to $\pm(2\text{–}3) \cdot 10^{-5}$ g·cm^{-3} [5]. In addition, due to the different inertia of temperature and conductivity sensors in layers with high gradients of these values the additional errors can be $\pm 3 \cdot 10^{-5}$ g·cm^{-3} [5]. The large dimensions of the conductivity sensors (up to 10 cm in diameter) do not make it possible to attain a high spatial resolution of the records.

An attempt to bypass the mentioned difficulties and obtain more precise information on the fine structure of the ρ field in situ was undertaken at the Institute of Oceanology P. P. Shirshov USSR Academy of Sciences. V. L. Vlasov constructed an instrument for measuring the fine structure of vertical density profiles of sea water density using data on the vertical stratification of the refractive index n of light in water. The basis for the instrument is the optical interferometry method, having a great speed, high sensitivity and broad dynamic range [6]. The change in the difference in the path of the light rays in the instrument Δz is associated with a change in the refractive index Δn and the length l of the instrument base by the simple expression:

$$\Delta z = \Delta n \, l = 1/2 \, \lambda \alpha, \tag{1}$$

where λ is the length of the light wave (in the described instrument equal to 6328 A -- the He-Ne line of the laser source); α is the relative shift of the interference bands (in fractions of band width).

The relationship between the ρ value and the refractive index n is stipulated by the Lorentz-Lorenz formula (for example, see [7]):

$$\rho = \frac{1}{k} \frac{n^2 - 1}{n^2 + 2}, \tag{2}$$

where k is specific refraction. Expanding the right-hand side of (2) into a series in the neighborhood of the point $n = n_0$ and leaving only the first two terms of the expansion, we obtain approximately

$$\Delta \rho / \rho_0 = a \Delta n, \tag{3}$$

where the coefficient $a = 6n_0/(n_0^2 - 1)(n_0^2 + 2)$. With a standard value $n_0 = 1.338$ and $\rho_0 = 1$ g·cm^{-3}, $\rho_0 a = 2.68$. Formula (3) makes it possible to determine $\Delta\rho$ with an accuracy $\sim 10^{-6}$ g·cm^{-3} if the absolute ρ change during the measurements does not exceed 10^{-2} g·cm^{-3}. Such a condition is satisfied in the overwhelming majority of regions in the world ocean since the change in water density with depth as a rule does not exceed the mentioned limit. It must be noted, however, that the proportionality factor k^{-1} in the Lorentz-Lorenz formula can have a weak dependence on T and S [8], as a result of which the error in determining $\Delta\rho$ can increase somewhat. However, at the present time reliable quantitative evaluations of this effect are lacking and therefore their allowance remains a matter of the future.

It follows from formulas (1) and (3) that the accuracy of the optical-interference method for determining Δn and $\Delta\rho$ is dependent on the length of the measurement base in the instrument and the accuracy in measuring the relative shift of the interference bands. For example, when $l = 1$ cm and the reading accuracy is $d \sim 0.005$ of the width of the interference band we find that the possible accuracies in determining Δn and $\Delta\rho$ in this case can attain values $\pm 1.6 \cdot 10^{-7}$ and $\pm 4.3 \cdot 10^{-7}$ g·cm^{-3} respectively. Such an accuracy in measuring α could be realized with temperature-vibrational interference always existing under natural conditions using the dynamic method of noise-immune remote measurements relative to the shift of two systems of interference bands proposed by V. L. Vlasov [9] and then improved in [10-12]. Earlier under special laboratory conditions (in thermostated and vibration-insulated rooms) and a static regime this accuracy did not exceed 0.1-0.05 of the width of the interference band [13].

A block diagram of the apparatus intended for measurement of the fine structure of the ρ field in the ocean is shown in Fig. 1. In the laser photoelectric interferometer a parallel light beam passes through the investigated medium and by means of two photomultiplier diaphragms (with diameters ~ 0.5 mm) the light rays, the difference in whose geometrical lengths is also the measurement base of the instrument, equal in our case to ~ 5 mm, are "cut" from it. These light rays interfere with the reference light beam and form two systems of interference bands, on which destabilizing factors exert an identical effect and thereby do not exert an influence on the accuracy in determining Δn. True, the reading accuracy in the described device is somewhat reduced due to the imperfection of digital-analog recorders (up to ± 0.05 of the band width when using a digital reversible recorder and up to ± 0.025 of the band width for an analog recorder). The accuracy in the Δn and $\Delta\rho$ readings is $\pm 3.1 \cdot 10^{-6}$ and $\pm 8.3 \cdot 10^{-6}$ g·cm^{-3} for the first case and $\pm 1.6 \cdot 10^{-6}$ and $\pm 4.3 \cdot 10^{-6}$ g·cm^{-3} for the second.

After the digital recorder, measuring whole and fractional parts of the band shift, and the analog device, measuring only fractional parts of the shift, the information is recorded on a high-speed recorder and automatically recording potentiometer and appears on a digital display. In the case of large "surges" of the $\Delta\rho$ values due to fine-structured peculiarities of the ρ field, in order to exclude ambiguity in the measurements with the analog

unit in a number of cases it was necessary to "coarsen" the interferometer response artificially; in this case the reading error was $\pm 1 \cdot 10^{-5}$ g·cm^{-3}. The inertia of the entire measurement channel was determined by the inertia of the automatic recorders and also by the parameters of the electric filters and was equal to $\sim$0.1 sec.

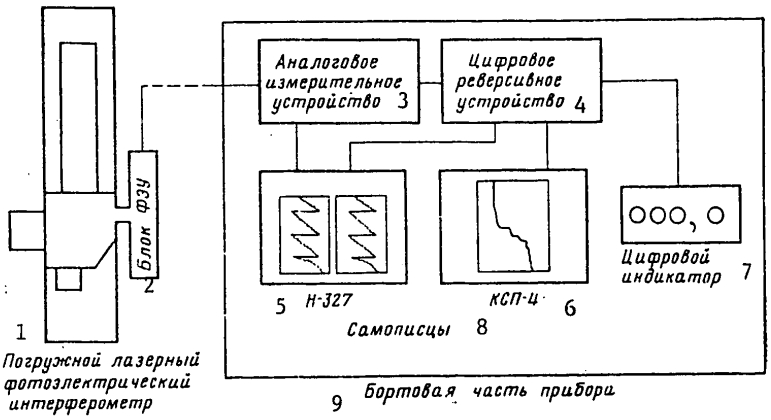

Fig. 1. Block diagram of apparatus for measuring the fine structure of the density field in the ocean by the optical-interference method.

KEY:

1. Submerged laser photoelectric interferometer
2. Unit of photomultipliers
3. Analog measuring device
4. Digital reversing unit
5. N-327
6. KSP-4
7. Digital indicator
8. Automatic recorders
9. On-board part of instrument

Figure 2 shows a vertical profile $\Delta\rho(z)$ obtained using the described instrument at station 1611 in the Philippine Sea on the 19th voyage of the scientific research vessel "Dmitriy Mendeleyev" [14]. The horizontal line corresponds to 0.1 of the width of the interference band, which is equal to double the error of the digital recording unit. The stepped structure of the $\Delta\rho(z)$ profile in layers with small vertical ρ gradients (to a depth of 70 m) falls within the limits of the mentioned error. In the deeper layers, where the density gradients are greater, the fine peculiarities of the profile are registered reliably. In particular, an interesting peculiarity of the $\Delta\rho(z)$ profile is the layer with a thickness of about 1 m shown in the inset in Fig. 2, in which one can see fine-structured peculiarities of

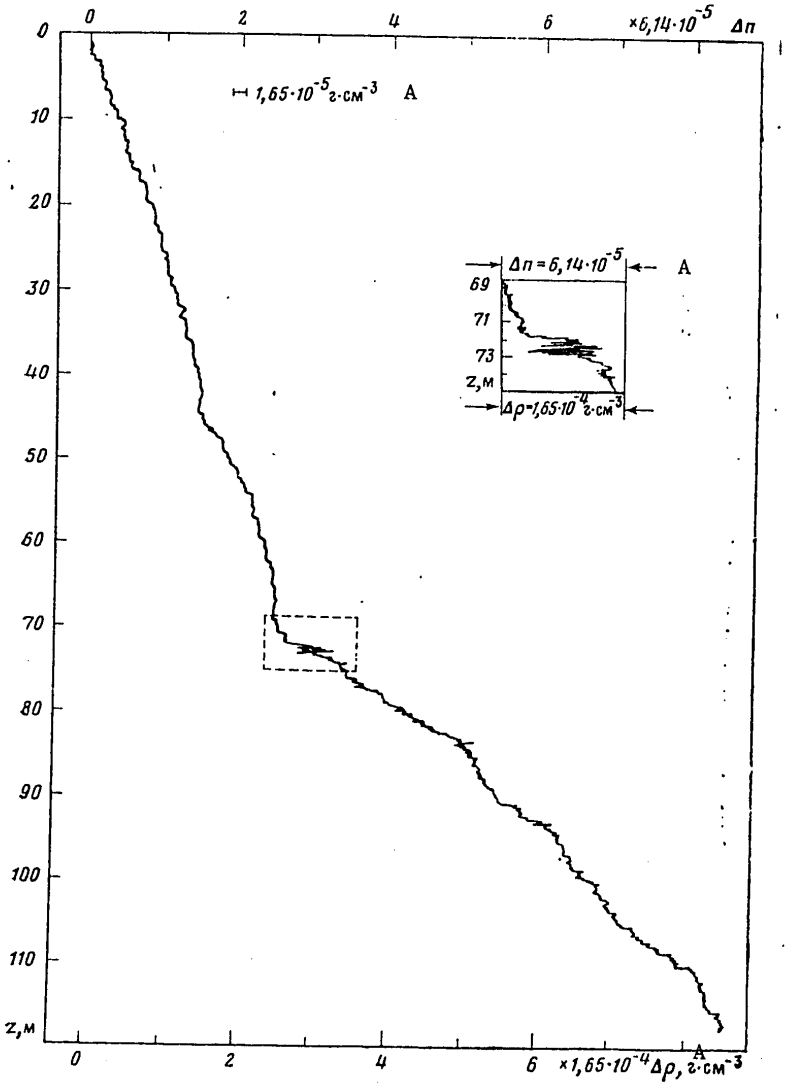

Fig. 2. Vertical profile of change in refractive index - density of sea water at station 1611 with coordinates 10°40'N, 126°45'E. A section of the profile within the dashed rectangle is shown separately.

KEY:

A) $g \cdot cm^{-3}$

the density field with vertical scales of only 5-10 cm and with inversion density gradients in them. It is interesting to note that similar inversion layers with a thickness of about 1 m were observed in approximately 10% of the cases on the $\Delta\rho(z)$ profiles obtained on a voyage at 11 stations in different regions of the world ocean. The internal fine structure of such layers was different, not always similar to that shown in Fig. 2. Evidently, the origin of such fine inversion layers in the density field in the ocean cannot be caused by local mechanisms of generation of field disturbances, for example, by instability of movements of waters of the Kelvin-Helmholtz type. As confirmation of such a conclusion we can use the similarity between the patterns of inversion layers in the ocean and data from laboratory experiments for investigating instability of Kelvin-Helmholtz movements. In the ocean a similar phenomenon was recently discovered by Gregg by indirect methods [15].

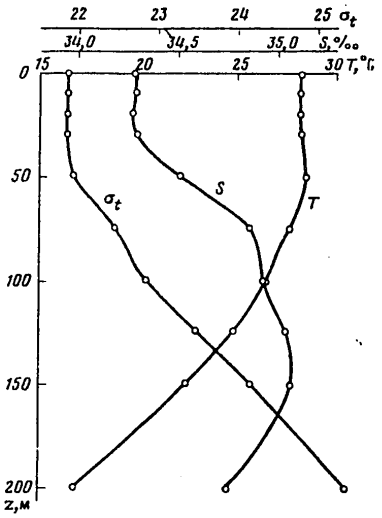

Fig. 3. Distribution of temperature T, salinity S and conditional density σ_t with depth at station 1606.

Series of six soundings were carried out on 25 September 1977 at station 1606 at a point with the coordinates 11°30'N, 129°45'E. The maximum depth of sounding with the interferometer was 120 m; the interval between soundings was 30 minutes. Sea waves did not exceed class 2; the wind was northwesterly, $\sim$4 m/sec; the vessel drifted toward the southwest at a speed of about 0.7 m/sec. The macroscale hydrological conditions at the station are given in Fig. 3. The upper mixed layer here had a thickness of about 50 m; the mean vertical density gradient in the layer from 50 to 200 m is close to $2.3 \cdot 10^{-5}$ g·cm^{-3}/m. All the profiles obtained at the station had a clearly expressed fine structure with vertical scales greater than 1 m.

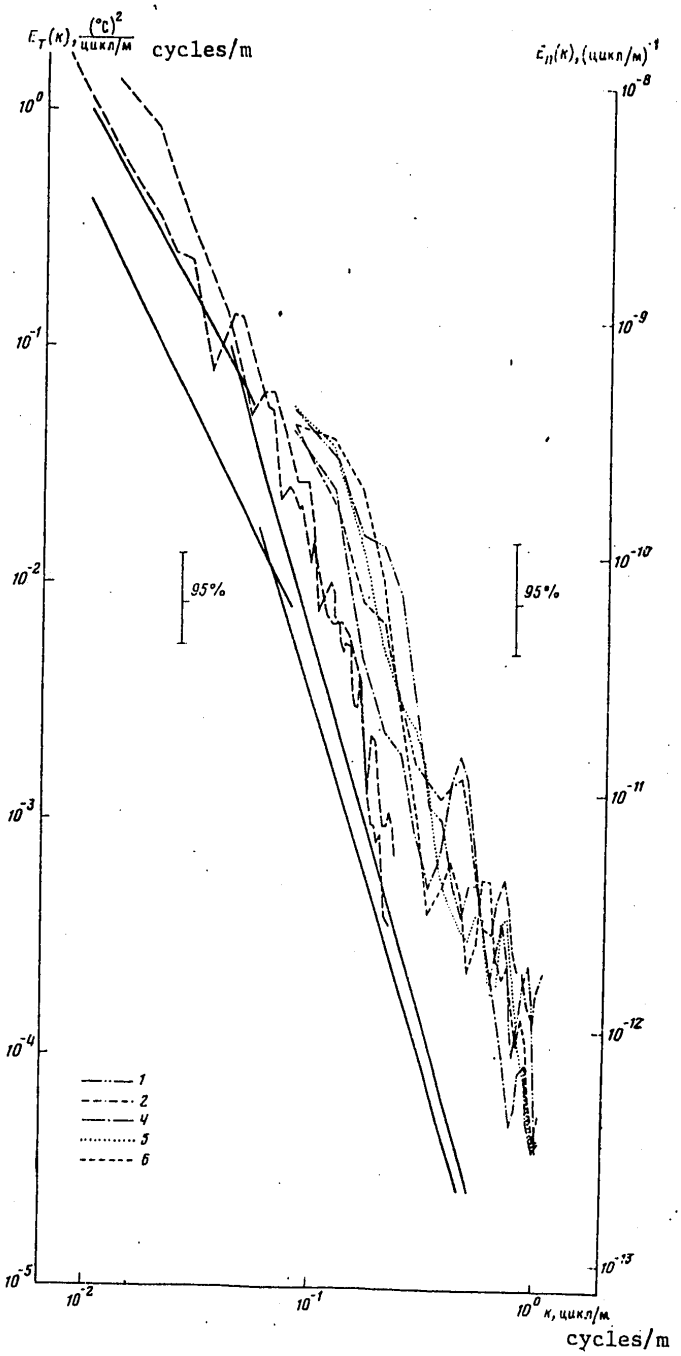

Fig. 4. Spectral densities of vertical inhomogeneities of refractive index of sea water for soundings 1, 2, 4, 5 and 6 at station 1606. The dashed and solid curves show the spectra of vertical temperature nonuniformities from [16] and [17] respectively. The vertical segments represent the 95% confidence intervals for spectra of the refractive index (at right) and temperature from [16] (at left).

The details of the fine structure were randomly deformed from one profile to another; therefore, a statistical analysis was made of them. The discretization of the profiles was carried out with a depth interval 0.48 m, which led to series with a length of 250 $\Delta\rho$ values for each sounding. A statistical analysis of the series was preceded by high-frequency filtering with the use of a cosine filter. Computations of the spectral densities of the filtered $\Delta\rho'(z)$ series were carried out using the Tukey method with 27 degrees of freedom.

The $E_\rho(k)$ spectra are given on a logarithmic scale in Fig. 4 for five soundings. The curves form a relatively dense beam of lines with "surges" not exceeding the 95% confidence interval, except for the peak on curve 4 with a value of the wave number k = 0.46 cycle/minute, which is evidently associated with the rolling of the ship. Since the fluctuations of the refractive index $\Delta n'$ and density $\Delta\rho'$ of water are influenced by fluctuations of both temperature and salinity, their relative contribution can be evaluated from the values of the gradients of the corresponding mean fields. At the considered station, according to Fig. 3, the main contribution to $\Delta n'$ and $\Delta\rho'$ must be from temperature pulsations. Accordingly, as a comparison Fig. 4 shows the spectra of the fine structure of the temperature field $E_T(k)$, computed using data from measurements in the Philippine Sea by a microstructure probe with a temperature sensor [16]. One of the $E_T(k)$ spectra was obtained in the layer from 0 to 300 m and the other in the layer 300-600 m. It follows from a comparison of the $E_\rho(k)$ spectra (reduced to units $(°C)^2$ $(cycles/m)^{-1}$) and $E_T(k)$ spectra that in the investigated layer of the ocean from 0 to 120 m the $\Delta n'$ and $\Delta\rho'$ pulsations evidently receive some contribution from salinity pulsations, since the $E_\rho(k)$ spectra are situated somewhat above the ET(k) curves.

Figure 4, as a comparison, schematically shows the spectra of the fine vertical structure of the temperature field in the main thermocline in two regions of the Pacific Ocean obtained by Gregg [17]. On these spectra there is a marked change in slopes for k values falling in the interval from 0.06 to 0.1 cycle/m, that is, in the range of scales from 10 to 17 m. With k less than the mentioned values the slope of the spectra is somewhat less than -2, whereas with greater k values the slopes become close to -3. Such a change in slope was caused, in Gregg's opinion, by the fact that in the larger-scale interval the main role is played by internal waves, and in the small-scale interval -- by the fine structure of the field itself. Such a point of view is confirmed, in particular, by an absence of coherence at scales less than 10 m for successively measured

(with an interval of 12 minutes) T(z) profiles [18].

The E_ρ (k) spectra constructed on the basis of our measurements (Fig. 4) are also characterized by a marked change in slope with a k value close to 0.12 cycle/m (the corresponding vertical scale of inhomogeneities is about 8 m). For disturbances of the density field with scales less than 8 m the E_ρ (k) spectral curves are well approximated by power-law expressions with an exponent close to -3, which agrees with data on the $E_T(k)$ spectra. However, the levels of the $E_T(k)$ spectra which we obtained are somewhat above the levels of the $E_T(k)$ spectra cited by Gregg.

Table 1

Mean Coherence Values Using Data from Multiple Sounding With Interferometer

Диапазон волновых чисел k, цикл/м 1	Диапазон масштабов, l_z, м 2	Временной сдвиг τ, ч 3			
		0,5	1,0	1,5	2,0
0,083÷0,12	12÷8,0	0,51	0,74	0,45	0,34
0,17÷0,29	6,0÷3,4	0,17	0,02	0,09	0,14
0,33÷0,62	3,0÷1,6	0,13	0,30	0,12	0,14
0,67÷1,0	1,5÷1,0	0,22	0,09	0,10	0,07

KEY:

1. Range of wave numbers h, cycles/m
2. Range of scales, l_z, m
3. Time shift τ, hours

Table 2

95% Confidence Intervals for Mean Coherence Values $\bar{K}$ and Phase Shift $\bar{\varphi}$ (in Degrees) for Significant Coherence Evaluations

Диапазон волновых чисел k, цикл/м 1	Диапазон масштабов l_z, м 2	Временной сдвиг τ, ч 3			
		0,5		1	
		$\bar{K}$	$\bar{\varphi}$	$\bar{K}$	$\bar{\varphi}$
0,083÷0,12	12÷8,0	0,39÷0,61	−23÷15	0,64÷0,81	−56÷−30
0,17÷0,29	6,0÷3,4	0,06÷0,27	−29÷77		
0,33÷0,62	3,0÷1,6	0,05÷0,20	111÷205	0,20÷0,38	130÷180
0,67÷1,0	1,5÷1,0	0,15÷0,28	−2÷44		
0,083÷0,12	12÷8,0	0,29÷0,59	−92÷−34	0,16÷0,50	−148÷−64
0,17÷0,29	6,0÷3,4				
0,33÷0,62	3,0÷1,6	0,03÷0,21	−2÷156	0,05÷0,23	−12÷102
0,67÷1,0	1,5÷1,0				

KEY: Same as Table 1

The data from multiple soundings with an interferometer at station 1606 were also used for computing the reciprocal statistical characteristics of the $\Delta\rho_i(z)$ records. A transformation of the $\Delta\rho(z)$ profiles from sounding to sounding can be regarded with a certain approximation as their temporal variability, since the wind drift of the ship is small and in the region of measurements in the upper 200-m layer of the ocean there is a current of westerly direction which is quasihomogeneous with depth [19]. Evaluations of the reciprocal statistical characteristics of the $\Delta\rho_i'$ profiles were computed for all possible pairs of i and j profiles (profile 3 was excluded from consideration due to gaps in the registry of signals). In order to check the hypothesis that the true coherence is equal to zero we used the criterion of significance of the coherence evaluation K_{ij} (for example, see [20]). In computing the phase shift φ_{ij} the confidence intervals were computed with a significance level β equal to 0.05, and for the Arth K_{ij} values such intervals were also evaluated with $\beta = 0.05$ using the expression $\pm(1 - \beta/2)\sqrt{\nu}$, where $N(1 - \beta/2)$ is the percentage point of a normal distribution with the significance level, β, ν is the number of degrees of freedom [20]. In order to reduce the scatter of individual K_{ij} and φ_{ij} evaluations we carried out averaging of the reciprocal co- and quadrature spectra and autospectra for all pairs of soundings spaced at identical time intervals τ. The averaging was also carried out within the limits of some defined ranges of wave numbers. The mean $\overline{K}(\tau)$ values obtained in this way are given in Table 1; the 95% confidence intervals of the mean coherence values and phase shift, taking into account the different number of degrees of freedom, are given in Table 2 for significant coherence evaluations. The ranges of wave numbers k and the corresponding l_z scales, indicated in Tables 1 and 2, are determined by their limiting discrete values, for which we computed the statistical characteristics of the $\Delta\rho_i'(z)$ series.

According to the data in Table 2, in all four ranges of wave numbers k (scale l_z) the coherence is significantly different from zero with a time shift $\tau = 0.5$ hour. In the case of greater τ values (up to 2 hours) the coherence is significant in the intervals of scales of inhomogeneities 1.6-3.0 m and 8.0-12 m; however, for other intervals the K function is close to zero. At the same time, in our opinion, the rolling of the vessel could exert an appreciable influence on the coherence value in the range 1.6-3.0 m; therefore, this range henceforth is not considered. The absence of coherence with $l_z < 8$ m for $\tau \geqslant 1$ hour indicates that the characteristic time of existence of nonuniformities of the density field with vertical scales $l_z < 8$ m fell in the interval 0.5-1 hour. The different behavior of the coherence values with an increase in τ for the ranges of scales of nonuniformities $l_z < 8$ m and l_z = 8.0-12 m indicates, evidently, different mechanisms of transformation of such inhomogeneities. At the limiting scale, close to 10 m, there is also a marked change in the spectral slopes $E_\rho(k)$ (Fig. 4). These facts make it possible to draw the quite sound conclusion that the variability of the vertical inhomogeneities of the density field with scales of 8-12 m in

the region of observations was caused by the effect of internal gravitational waves.

An interesting peculiarity of the $\overline{K}(\tau)$ dependence for the range of scales l_z = 8.0-12 m is a statistically guaranteed maximum with τ = 1 hour. The possibility of the appearance of relative maxima on the $\overline{K}(\tau)$ curve with an increase in τ is suggested by the Garrett and Munk model of internal waves [21], who obtained such a result for the coherence of vertical displacements of isopycnic surfaces in the ocean. With a constant density gradient this profile evidently is proportional to the profiles of density disturbances $\Delta\rho'(z)$ considered in this study. The effect of internal waves must be manifested in the function $\overline{K}(\tau)$ by the periodic appearance of maxima with a further increase in τ. Unfortunately, available experimental data at the present time afford no possibility for tracing the behavior of the $\overline{K}(\tau)$ function in the case of large τ values. The collection of such material and its analysis is a matter for future investigations.

We take the opportunity to thank A. K. Ambrosimov for participating in the preparation of the apparatus for work and carrying out the measurements and also in preparation of data for input into an electronic computer.

BIBLIOGRAPHY

1. Horn, R., MORSKAYA KHIMIYA (Marine Chemistry), "Mir," 1972.

2. OKEANOGRAFICHESKIYE TABLITSY (Oceanographic Tables), Gidrometeoizdat, 1975.

3. Defant, A., PHYSICAL OCEANOGRAPHY, 1, Pergamon Press, Oxford, 1961.

4. Chen, C. T., Millero, F. J., "Precise Equation of State of Sea Water for Oceanic Ranges of Salinity, Temperature and Pressure Parameters," DEEP SEA RES., 24, 365-369, 1977.

5. Ginzburg, A. I., Derevshchikov, P. A., Prokhorov, V. I., "Principles for Constructing Sounding Apparatus for Studying the Fine Structure of Ocean Waters," MEZOMASSTABNAYA IZMENCHIVOST' POLYA TEMPERATURY V OKEANE (Mesoscale Variability of the Temperature Field in the Ocean), IOAN SSSR, 101-108, 1977.

6. Barber, G. J., "An Optical Interferometer Method of Calibrating a Crystal Gauge for the Measurement of Sound Wave Transients," J. SCI. INSTRUMENT., 32, No 1, 7-8, 1955.

7. Born, M., Wolf, E., OSNOVY OPTIKI (Principles of Optics), "Nauka," 1970.

8. Stanley, E. M., "The Refractive Index of Sea Water as a Function of Temperature, Pressure and Two Wavelengths," DEEP SEA RES., 18, 833-840, 1971.

9. Vlasov, V. L., "Method for Measuring the Fractional Part of the Shift of Two Systems of Interference Bands in Special Interferometers and an Apparatus for Implementing This Method," Author's Certificate No 124676, BYULL. IZOBR. (Bulletin of Inventions), No 23, 1959.

10. Vlasov, V. L., Medvedev, A. N., "Apparatus for Measuring the Fractional Part of the Shift of Two Systems of Interference Bands," Author's Certificate No 509767, BYULL. IZOBR., No 13, 1976.

11. Vlasov, V. L., Medvedev, A. N., "Precise Measurement of the Fractional Part of the Relative Shift of Two Systems of Interference Bands," PRIBORY I TEKHNIKA EKSPERIMENTA (Experimental Instruments and Techniques), No 4, 198-200, 1972.

12. Vlasov, V. L., Medvedev, A. N., "Photoelectric Method for Precise Measurement of Small Relative Shifts of Two Systems of Interference Bands," IZMERITEL'NAYA TEKHNIKA (Measurement Technology), No 8, 47-49, 1975.

13. Kondrashkov, A. V., INTERFERENTSIYA SVETA I YEYE PRIMENENIYE V GEODEZII (Interference of Light and its Use in Geodesy), Geoizdat, 1956.

14. Ozmidov, R. V., "19th Voyage of the Scientific Research Vessel 'Dmitriy Mendeleyev'," OKEANOLOGIYA (Oceanology), 18, No 3, pp 564-568, 1978.

15. Gregg, M. C., "Variations in the Intensity of Small-Scale Mixing in the Main Thermocline," J. PHYS. OCEANOGR., 7, No 3, 436-454, 1977.

16. Korchashkin, N. N., Lozovatskiy, I. D., Ozmidov, R. V., "Variability of the Fine Vertical Structure of the Temperature Field in the Western Part of the Pacific Ocean," OKEANOLOGIYA, 19, No 2, 197-205, 1979.

17. Gregg, M. C., "A Comparison of Fine-Structure Spectra from the Main Thermocline," J. PHYS. OCEANOGR., 7, No 1, 33-40, 1977.

18. Hayes, S. P., "Preliminary Measurements of Time-Lagged Coherence of Vertical Temperature Profiles," JGR, 80, 307-311, 1975.

19. Burkov, V. A., "Circulation of Waters in the Northern Part of the Pacific Ocean," OKEANOLOGIYA, 3, No 5, 1963.

20. Jenkins, H., Watts, D., SPEKTRAL'NYY ANALIZ I YEGO PRILOZHENIYA (Spectral Analysis and its Applications), No 2, "Mir," 1972.

21. Garrett, C. J. R., Munk, W. H., "Space-Time Scales of Internal Waves: A Progress Report," JGR, 80, 291-297, 1975.

[19-5303]
5303/CSO: 1866

UDC 551.46.07.660.3

FIRST VOYAGE OF HYDROGRAPHIC SHIP 'GEORGIY MAKSIMOV'

Moscow OKEANOLOGIYA in Russian Vol 19, No 4, 1979 pp 749-751

[Article by G. B. Udintsev and N. I. Pavlenkova: "First Voyage of the Hydrographic Ship "Georgiy Maksimov" Under the Program of the Institute of Physics of the Earth imeni O. Yu. Shmidt USSR Academy of Sciences"]

[Text] During the period 7 December 1978 - 6 April 1979 there was an expeditionary voyage of the hydrographic ship "Georgiy Maksimov" of the Hydrographic Station at Provideniya of the Hydrographic Enterprise of the USSR Merchant Marine Ministry, leased by the Institute of Physics of the Earth imeni O. Yu. Shmidt USSR Academy of Sciences for carrying out comprehensive geophysical investigations of the earth's crust and upper mantle in the oceans. This was the first voyage of the vessel under the five-year program for investigating the floor of the world ocean by the Institute of Physics of the Earth for studying the problem of tectonic nonuniformity of the oceanic regions of the earth and the problem of the nature of the ocean-continent boundary, its spatial and temporal position. The principal task of the expedition was to obtain a complex of geophysical data characterizing some highly important tectonic structures on the floor of the Indian Ocean which are of interest for understanding the role of different tectonic processes in the development of oceanic regions.

The hydrographic ship "Georgiy Maksimov" belongs to a series of ships of the "Dmitriy Ovtsyn" class. It has a displacement of 1,600 tons, has good seagoing qualities and is outfitted with modern navigational equipment, including satellite navigation apparatus. The ship's maximum speed is 12 knots. In order to carry out the complex of geophysical investigations the ship was supplied with temporarily installed apparatus, including instruments for continuous seismic profiling, a magnetometer survey, pneumatic sound sources for deep seismic sounding and bottom seismic stations. The expedition was organized by the Institute of Physics of the Earth with participation of specialists of the Institute of Terrestrial Magnetism, Ionosphere and Radio Wave Propagation USSR Academy of Sciences, the Pacific Ocean Oceanological Institute Far Eastern Scientific Center USSR Academy of Sciences, Moscow State University imeni M. V. Lomonosov and the Hydrographic Enterprise of the USSR Merchant Marine Ministry. Also participating in the expedition were

Japanese scientists from Toki University (Shizuoka) M. Hoshino and M. Shiba and the Australian scientist B. D. Johnson from Macquarie University (Sydney). G. B. Udintsev and N. I. Povlenkova headed the expedition in different stages of the voyage.

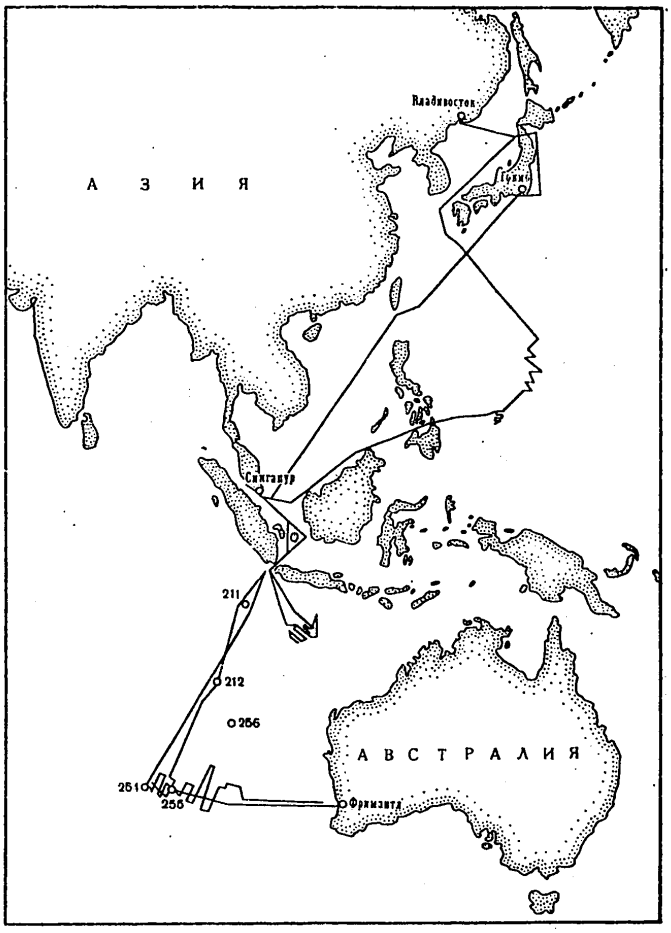

Map of track of hydrographic ship "Georgiy Maksimov" on the first voyage under the program of the Institute of Physics of the Earth. The figures correspond to the numbers of boreholes drilled by the ship "Glomar Challenger" to which the geophysical survey by the "Georgiy Maksimov" was tied in.

The expedition began with departure from the port of Vladivostok on 7 December 1978. After passing through the Sea of Japan, Tsushima Strait and the East China Sea, the ship entered the Philippines basin of the Pacific Ocean

and carried out a detailed comprehensive geophysical survey in the Yap fault zone and in one of the sectors of the Kyushu-Palau submarine ridge (see figure). Thereafter the "Georgiy Maksimov" passed through the Philippine Basin and the Sulu Sea and the South China Sea to the port of Singapore. From this port, after replenishing supplies of fuel, water and food, the ship passed through Sunda Strait into the Indian Ocean into the region of the Rua submarine rise, lying at the edge of the floor to the south of the Sunda trench. Here a regional comprehensive geophysical survey was carried out, seismological observations were carried out for a period of a week using bottom seismic stations and deep seismic sounding was carried out along 200 km of profiles. Upon completion of this complex of investigations the ship again called at the port of Singapore for a partial replacement of scientific personnel.

From Singapore the "Georgiy Maksimov" again headed through the Sunda Strait into the southern part of the Indian Ocean, into the region of the joining of the East Indian Ocean and West Australian submarine ridges. Here it carried out a comprehensive regional geophysical survey of the West Australian Ridge along a system of parallel runs oriented across the strike of the ridge. The length of the runs was from 200 to 300 miles and the distance between them was 30-40 miles. These survey runs in the south took in the periphery of the Australian-Antarctic Ridge, intersected the West Australian Ridge and emerged on the floor of the West Australian and Naturalist Basins. There was a total of 10 intersections of the West Australian Ridge. In the course of this survey the vessel called at the Australian port of Fremantle for replenishing supplies and making scientific contacts with Australian scientists in Perth. In the course of the geophysical survey there were also seismological observations using bottom seismic stations, put in place for a week, and deep seismic sounding along profiles with a total extent of more than 300 km. Upon completing work in the region of the West Australian Ridge the vessel passed along a profile through the West Australian Basin. The geophysical survey made at this time was tied in to abyssal drilling boreholes, as in the regional survey of the West Australian Ridge. The "Georgiy Maksimov" passed through the Sunda Strait from the Indian Ocean and arrived at the port of Singapore where the ship left some of the participants on the expedition. Then passing through the South China Sea, Luzon Strait and the Philippine Basin of the Pacific Ocean, the "Georgiy Maksimov" arrived in the port of Tokio for the purpose of replenishing supplies and making contacts with Japanese scientists. The expedition ended with arrival in the port of Vladivostok on 6 April 1979.

The work of the first voyage of the "Georgiy Maksimov" under the program of the Institute of Physics of the Earth was a logical continuation of the investigations initiated by our group as early as 1964-1965 during the 36th voyage of the "Vityaz'." The work rested on a generalization of the materials of geological-geophysical investigations of preceding years which we carried out during compilation of the international GEOLOGO-GEOFIZICHESKIY ATLAS INDIYSKOGO OKEANA (Geological-Geophysical Atlas of the Indian Ocean), (1975), on the results of abyssal ocean drilling carried out by the drilling ship "Glomar Challenger," and also the results of drilling on the submarine margin of the Australian continent, carried out by industrial companies.

The expedition collected extensive materials on the geophysics and structure of the floor of the eastern part of the Indian Ocean, and also for individual regions of the Pacific Ocean. The most important results are those from regional investigations of the West Australian Ridge and the Rua Rise in the Indian Ocean.

For the first time the morphology of the West Australian Ridge was established with sufficient clarity and a detailed study was made of the structure of the sedimentary layers covering it and the morphostructure of its acoustic basement. For the first time a study was also made of the seismicity of this ridge. There was supplementation of the earlier fragmentary data on the deep structure of the ridge obtained by means of deep seismic sounding. On the crest of the ridge a study was made of two earlier uninvestigated seamounts for which names were proposed: Akademik Gamburtsev (30°03'S and 88°52'E) and Akademik Rem Khokhlov (31°24'S and 94°53'E). Significant differences were found in the tectonics of the West Australian Ridge and the periphery of the Australian-Antarctic Ridge adjacent to it on the south, reflecting, so it seems to us, not only differences in age, but also in the very nature of these structures. The echelon-oriented system of trenches and faults bounding the West Australian Ridge on the south, it is becoming clear, is a characteristic peculiarity of the northern margin of the Australian-Antarctic Rise. This system of faults is also traced eastward, to the south of the Naturaliste Plateau. The structures of the sedimentary cover and the acoustic basement of the West Australian Ridge, detected by means of seismic profiling, in combination with data from abyssal drilling, indicate that the ridge has experienced differentiated vertical movements. The structural unity of the West Australian Ridge and the part of the bed of the West Australian ocean basin adjoining it on the north was established. On the northern slope of the West Australian Ridge and in the adjacent part of the West Australian Basin it was possible to detect diapir structures making it possible to re-evaluate the possible prospects for finding petroleum and gas in the open regions of the ocean.

The Rua Rise is a massive arched structure with an asymmetric profile -- with a relatively gentle slope in the direction of the Sunda trench and steeper in the direction of the ocean floor. The sedimentary layer covering it has the greatest thicknesses in the arched part of the rise. Along the western margin of the rise there are several seamounts evidently of volcanic origin and associated with a fault zone of southwesterly strike. One of these mountains was discovered for the first time and was investigated by the expedition. Plans call for assigning the name of the outstanding Soviet geophysicist Fedynskiy. The peak of this seamount lies at the point 13°45'S and 108°45'E. About 100 earthquakes were registered during the seven days of the seismological observations.

The work of the first voyage of the "Georgiy Maksimov" will be continued in the course of comprehensive geological-geophysical investigations and a lithospheric seismic experiment on the East Indian Ocean geotraverse;

planned by the Institute of Physics of the Earth imeni O. Yu. Shmidt, in the coming five-year period.

5303
CSO: 1866

UDC 551.46

MONOGRAPH ON ADVANCES IN SOVIET OCEANOLOGY

Moscow USPEKHI SOVETSKOY OKEANOLOGIYA (Advances in Soviet Oceanology) in Russian 1979 signed to press 13 April 79 pp 2, 157

[Annotation and table of contents from collection of articles edited by Academician L. M. Brekhovskikh, signed to press 13 Apr 79, 168 pages]

[Text] This collection of articles gives materials from the First Congress of Soviet Oceanologists. The articles are devoted to highly important aspects of modern oceanology -- physics, biology, chemistry and geology of the seas and oceans. Considerable attention is devoted to the problems involved in climatology and the problems in exploitation of the mineral resources of the floor. The papers cover the principal achievements of Soviet scientists in study and exploitation of the world ocean in the interests of the national economy of the country.

CONTENTS Page

Page

5303
CSO: 1865

UDC 551.465.11

MESOSCALE DYNAMIC PROCESSES IN THE OCEAN CREATED BY THE ATMOSPHERE

Moscow SREDNEMASSHTABNYYE DINAMICHESKIYE PROTSESSY OKEANA, VOZBUZHDAYEMYYE ATMOSFEROY (Mesoscale Dynamic Processes in the Ocean Created by the Atmosphere) in Russian 1979 signed to press 20 Feb 79 pp 2, 180-181

[Annotation and table of contents from book by S. S. Lappo, 181 pages]

[Text] Materials of intermittent observations of the variability of the level and current in regions of the ocean subjected to powerful synoptic atmospheric processes are analyzed.

The spatial characteristics of mesoscale atmospheric processes for the northern parts of the Atlantic Ocean, Pacific Ocean and Indian Ocean are examined on the basis of statistical charting of the fields of atmospheric pressure as a result of which there was found to be variability of level and sea currents caused by the atmosphere.

Peculiarities of forced mesoscale level variations are analyzed theoretically and factors which lead to nonstatic reaction of the open ocean to moving pressure formations and the transfer of mechanical energy from the atmosphere into the ocean in the region of mesoscales are evaluated. A relative picture of thermal and dynamic phenomena in the ocean on the basis of energy evaluations is presented.

The book is intended for scientists, graduate students and undergraduate students -- marine physicists, oceanologists and geophysicists.

CONTENTS Page

[34-5303]

5303/CSO: 1865

SEMINAR ON 'FUNDAMENTAL PROBLEMS OF ELECTROMAGNETIC RESEARCH AT SEA'

Moscow GEOMAGNETIZM I AERONOMIYA in Russian Vol 19, No 5, 1979 p 953

[Article by A. N. Pushkov]

[Text] During the period 19-23 February 1979 a seminar on "Fundamental Problems of Electromagnetic Research at Sea" was held at the Institute of Terrestrial Magnetism, Ionosphere and Radio Wave Propagation. The seminar was attended by 120 representatives from 28 organizations. The following problems were examined at the seminar:

1. The development of marine magnetometric apparatus for carrying out surveys and study of variations of the electromagnetic field.

2. Use of available information on the spatial-temporal structure of the geomagnetic field for studying the internal structure of the earth and the history of formation of the outer magnetically active shell.

3. Investigations of the variable electromagnetic field in the seas and its study for the purpose of electromagnetic sounding and profiling of the lithosphere and asthenosphere beneath the ocean.

The seminar noted the necessity for the speediest possible development and practical introduction of bottom component stations developed at the Institute of Terrestrial Magnetism, Ionosphere and Radio Wave Propagation and other organizations for sea electromagnetic investigations, making it possible to take variations into account in sea magnetic surveys, and what is more important, begin the introduction of methods for electromagnetic sounding and profiling. Simultaneously with the development of experimental investigations the seminar notes the importance of the work begun on developing a method for solving direct and inverse problems in electromagnetic sounding.

The Institute of Oceanology presented a series of reports written on the basis of the results of component and modular surveys carried out in 1978. It was possible to obtain the results in such a short time due to the routine processing of data on an electronic computer during the voyage. The seminar recommends the speediest possible introduction of this method at other organizations.

Great interest was shown in a world schematic map of the anomalous field prepared by a group of authors. It generalizes ideas concerning the anomalous field on the continents (in the form of isolines) and for the oceans (in the form of anomaly axes).

The seminar notes that for the development of generalizing investigations of the structure of the permanent field it is necessary to create a unified catalogue of data from sea magnetic surveys.

A resolution was passed calling for publication of the reports in the form of an individual collection.

5303
CSO: 1865

II. TERRESTRIAL GEOPHYSICS

Translations

UDC 550.837.1(470.21)

DEEP ELECTROMAGNETIC SOUNDING WITH A MAGNETOHYDRODYNAMIC GENERATOR ON THE KOLA PENINSULA

Moscow DOKLADY AKADEMII NAUK SSSR in Russian Vol 247, No 3, 1979 pp 578-582

[Article by Corresponding Member USSR Academy of Sciences G. I. Gorbunov, I. V. Bel'kov, V. I. Pavlovskiy, A. A. Zhamaletdinov, P. L. Katseblin, Yu. P. Kachayev, Academician Ye. P. Velikhov, Yu. M. Volkov, Yu. A. Dreyzin, Yu. I. Kuksa, A. V. Zotov, V. V. Yevstigneyev, A. S. Lisin, Academician B. P. Zhukov, V. V. Vengerskiy and Yu. P. Babakov, Kola Affiliate imeni S. M. Kirov, USSR Academy of Sciences, Apatity Murmanskaya Oblast]

[Text] A fundamental problem in modern geology is the formulation of a physical model of the earth. The principal role in its solution is played by geophysical research methods, and in particular, deep electromagnetic soundings (DES). Data on conductivity of deep horizons make it possible to judge the geothermal regime and mineralogical composition of the earth's deep layers [1, 2].

The most reliable information on the geoelectric cross section is given by sounding with artificial sources: they make it possible to carry out a more precise quantitative interpretation and more fully take into account the influence of horizontal inhomogeneity of the rocks. This direction in deep research, substantiated by Soviet geophysicists [3], is being broadly developed in the USSR and abroad. However, the further broadening of the possibilities of DES is limited by the absence of adequately powerful mobile electromagnetic field sources.

New possibilities are being afforded by the use of autonomous pulsed magnetohydrodynamic (MHD) generators capable of developing a power of about 100 MW in the emitting dipoles [4]. The first experiments in this direction were carried out in the Pamir [5] and in the Ural [6].

An experiment with DES on the Kola Peninsula has been carried out since late 1976. The attained range of signal registry is 750 km. The principal observations have been made with spacings up to 400 km. The energy source is a paired MHD generator (Fig. 1). Each such generator consists of three principal units: plasma generator, MHD channel and nonferrous

electromagnet. In the plasma generator there is combustion of a special solid fuel with an easily ionizing addition of an alkaline metal. In the MHD channel a supersonic plasma flow, formed by combustion products, is slowed under the influence of the electromagnet's field; in this way the kinetic energy of the plasma is transformed into an electric current, fed from electrodes installed along the lateral walls of the channel. The current is fed into the electromagnets at the initial moment from the capacitors in the excitation system. Subsequently one of the channels passes into a regime of autoexcitation and feeds an electric current into the windings of both electromagnets, whereas the energy of the second channel is entirely expended on maintaining the current in the load.

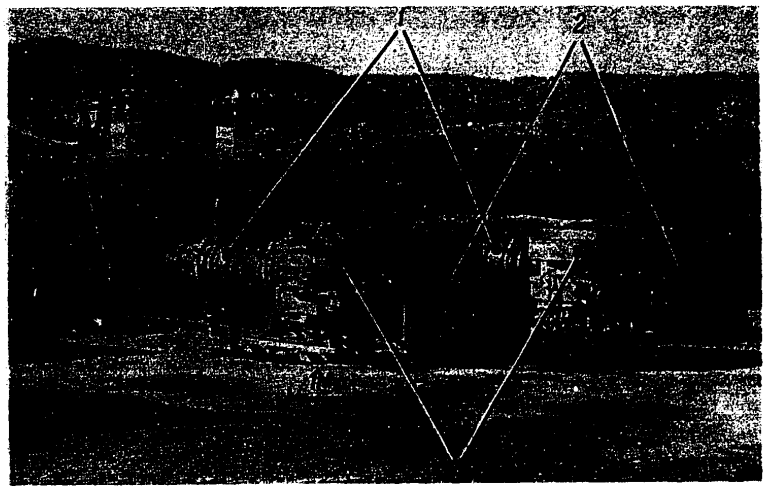

Fig. 1. "Khibiny-1" MHD apparatus on Sredniy Peninsula; 1) plasma generators; 2) MHD channels; 3) electromagnets.

A distinguishing characteristic of the experiment is the use of the bays and sea basin around the Sredniy and Rybachiy Peninsulas as a natural current circuit. The load resistance in this case was 90 megohm, of which 30 are accounted for by an aluminum cable weighing 160 tons, connecting Motovskiy and M. Volokovoy Bays. The maximum current in the load attains 22 kA. Pulse duration is 5-6 sec. The equivalent magnetic moment of the source thus employed, according to experimental estimates, was 10^{14} A·m^2.

Measurements of the source field were made over the entire territory of the Kola Peninsula and partially in Karelia using standard-produced MTL-71, TsES-1 and TsES-2 stations reequipped for the reception of individual

signals. Five field components were registered: E_x, E_y, H_x, H_y and H_z -- in the frequency range 0-1 Hz.

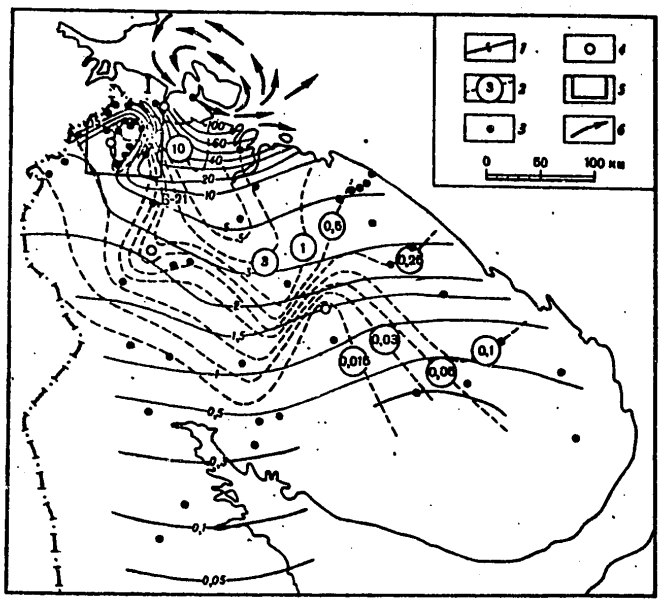

Fig. 2. Map of field isolines with distribution of observation points. Isolines: 1) E_r in V/km, 2) H_z in γ; observation points: 3) fundamental, 4) control; 5) area of detailed work in Pechenga region; 6) direction of electric currents in sea.

The processing of the measured signals was carried out by computing the Fourier spectra and their subsequent normalization using the spectrum of the current in the supply circuit, which makes it possible to regard this method as a modification of frequency sounding.

The investigated region consisted of ancient crystalline rocks of Archean and Proterozoic ages. The resistivity of most types of rocks varies in the range 10^4-10^5 ohm·m. The crystalline rocks were covered by moraine ($\rho \sim 10^3$ ohm·m, thickness 0-30 m). Neglecting its influence and for the time being not taking into account the possible increase in the conductivity of rocks with depth, it can be assumed that the depth of penetration of the electromagnetic field with a duration of the impulses of 5-6 sec in the investigated region is not less than 100-150 km. A serious circumstance complicating the use of DES on the Kola Peninsula is the broad development of formations with type-n conductivity [7, 8]. Spatially and genetically they are associated with major structural geology zones which are promising

in the search for minerals, such as the Pechengskaya, Imandra-Varzugskaya and other zones.

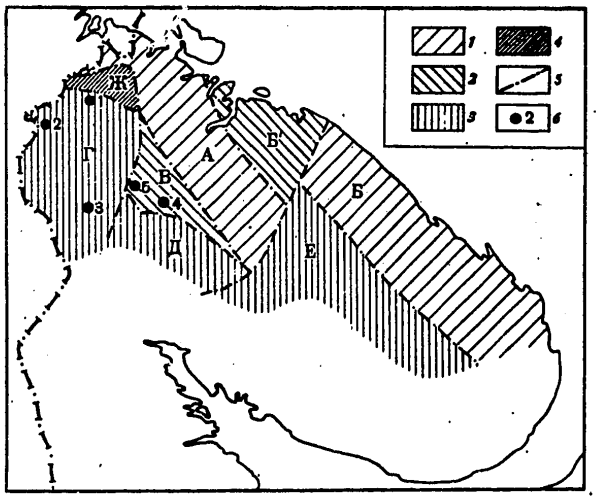

Fig. 3. Blocks with different resistivity of the earth's crust on the Kola Peninsula according to data from an experiment with a MHD generator (ohm·m): 1) 10^5, 2) 10^4, 3) 10^3, 4) 10^2 or less; 5) boundaries of blocks; 6) sounding points. Designations of blocks: A) Tsentral'no-Kol'skiy, Б and Б') Murmanskiy, B) Notozerskiy, Г) Allarechensko-Sal'notundrovskiy, Д) Monchegorskiy, E) Keyvskiy, Ж) Pechengskiy

The principal objective of the experiment is a clarification of a model of the earth's conductivity at depths of 20-100 km. The timeliness of the problem is determined by the fact that precisely in this depth range the information on the section is most contradictory. In particular, at these depths it is assumed that there is an intermediate conducting layer [9, 10], sometimes identified with the heated asthenosphere [11]. Under the conditions of an open crystalline shield, where unconsolidated screening deposits are absent, there is a possibility of giving the most definite answer to this question, taking the lateral influence of the structures into account.

Another problem, also to be solved within the framework of the experiment, is areal geoelectric mapping of the entire Kola Peninsula in the field of one source. This will create a possibility for detecting major conducting blocks in the earth's crust, which can be classified as ore fields, and also to detect deep faults.

The principal results of the experiment, based on data collected up to the present time, can be summarized as follows.

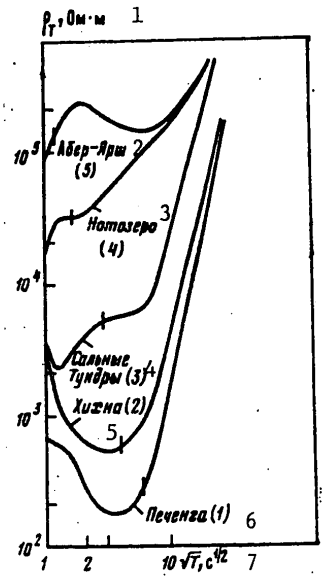

Fig. 4. Sounding curves $\rho_{T\ eff}$ based on data from spectral processing of pulsed signals of MHD generator. The vertical lines on the curves indicate the limits of the zone where $H_T(\omega)/H_Z(\omega) > 1$. The siting of the points is shown in Fig. 3.

KEY:

1. ohm/m
2. Ader-Yarsh
3. Notozero
4. Sal'nyye Tundry
5. Khikhna
6. Pechenga
7. $sec^{1/2}$

1. A map of division of the earth's crust on the Kola Peninsula into blocks with different resistivity (Fig. 3) was constructed on the basis of isoline maps of magnetic and electric fields (Fig. 2). Confirmation was obtained for the ideas expressed earlier in [7, 8] that blocks of the crystalline basement occupied by a thin network of n-type conductors are major (about 10^4 km^2) conducting sectors of the earth's crust ($\rho = 10^2$–10^3 ohm·m). A high resistivity (about 10^5 ohm·m) is characteristic of the Murmanskiy and Tsentral'no-Kol'skiy blocks.

2. Within the limits of the Murmanskiy block there was the most monotonic dropoff of the electric and magnetic fields, indicating an adequately uniform structure of the upper part of the earth's crust in this region and the favorableness of the conditions for carrying out DES. The influence of the shore effect, noted clearly in the behavior of the H_Z component (Fig. 2), agrees well with the results of modeling carried out taking into

account the finite conductivity of the sea. The most general analysis of attenuation of the electromagnetic field with increasing distance from the source makes it possible to draw the conclusion that there is no appreciable decrease in rock resistivity to depths of 30-40 km. In order to judge the nature of the section at greater depths it is necessary to carry out additional work for making the network finer and taking into account the lateral influence of the sea and rocks of the Keyv structural zone.

3. In the northwestern part of the Kola Peninsula, where rocks with n-type conductivity are widely developed, the structure of the electromagnetic field is deformed, approaching the form of a plane wave ($H_r/H_z \gg 1$). This makes it possible to carry out processing making use of impedance concepts, without taking source parameters into account. Figure 4 shows the constructed $\rho_{T\ eff}$ curves. Using the coordinates of the minima it is possible to estimate the total longitudinal conductivity S of the upper layer. The determined estimates vary from 150 mho for the southern margin of Pechenga to tens of mho in the Sal'nyye Tundry region.

4. The increased density of the observation network used in the Pechenga region (Fig. 2) demonstrated the possibility of using the "Khibiny" MHD apparatus for studying the internal structure of ore fields and for a joint analysis of the results with data from deep and superdeep drilling.

Thus, as a result of implementation of the first stage in the work it was possible to create a unique source of an electromagnetic field exceeding by 4-5 orders of magnitude the parameters of all apparatus used earlier. Methods were developed for measurement and analysis of the pulsed signals of the MHD generator and the first geological results characterizing the electric properties of the earth's crust on the Kola Peninsula were obtained.

BIBLIOGRAPHY

1. Noritomi, K., J. MINING COLL. AKITA UNIV., A1, 1, 27, 1961.

2. Lyubimova, Ye. A., Fel'dman, I. S., KORA I VERKHNYAYA MANTIYA ZEMLI (The Earth's Crust and Upper Mantle), Moscow, Izd-vo MGU, No 2, p 144, 1975.

3. Krayev, A. P., Semenov, A. S., Tarkhov, A. G., RAZVEDKA I OKHRANA NEDR (Prospecting and Conservation of Mineral Resources), No 3, 40, 1947.

4. Velikhov, Ye. P., Volkov, Yu. M., et al., TR. VI MEZHDUNARODN. KONFERENTSII PO MGD-GENERATORAM (Transactions of the Sixth International Conference on MHD Generators), Washington, 9-13 June 1975, Vol 5, p 211, 1975.

5. Velikhov, Ye. P., Volkov, Yu. M., et al., ISPOL'ZOVANIYE IMPUL'SNYKH MGD-GENERATOROV DLYA GEOFIZICHESKIKH ISSLEDOVANIY I PROGNOZA ZEMLETRYASENIY (Use of Pulsed MHD Generators for Geophysical Research and Earthquake Prediction), Moscow, 1975.

6. Astrakhantsev, G. V., Babakov, Yu. P., et al., DAN (Reports of the USSR Academy of Sciences), Vol 237, No 4, 808, 1977.

7. Semenov, A. S., VESTN. LGU (Herald of Leningrad State University), No 12, 19, 1970.

8. Zhamaletdinov, A. A., Semenov, A. S., Veselov, I. N., VESTN. LGU, No 18, 55, 1970.

9. Berdichevskiy, M. N., Borisov, V. P., et al., IZV. AN SSSR, FIZIKA ZEMLI (News of the USSR Academy of Sciences, Physics of the Earth), No 10, 633, 1969.

10. Porath, H., STRUCTURE AND PHYSICAL PROPERTIES OF THE EARTH'S CRUST, Washington, p 127, 1972.

11. Krasnobayeva, A. G., Kormil'tsev, V. V., Shepeleva, I. M., TEORIYA I PRAKTIKA ELEKTROMETRII (Theory and Practice of Electrometry), Sverdlovsk, p 21, 1972.

[0127-5303]

5303
CSO: 8144

UDC 550.814

REMOTE METHODS FOR STUDYING THE GEOLOGICAL STRUCTURE OF PETROLEUM AND GAS REGIONS

Moscow VESTNIK AKADEMII NAUK SSSR in Russian No 10, 1979 pp 69-78

[Article by Candidate of Geological-Mineralogical Sciences V. I. Gridin and Doctor of Geological-Mineralogical Sciences N. A. Yeremenko]

[Text] The increase in the demand for different types of mineral raw material, especially petroleum and gas, during recent decades has led to the development of new, high-altitude aerial and space methods for studying the earth's natural resources. Such remote study of the geological structure of petroleum and gas regions has at its basis the close interrelationships among the processes transpiring in the earth's crust and at the earth's surface, the manifestation of this natural pattern in the modern landscape and the objective reflection of the peculiarities of the latter in remote sensing materials. There is now no doubt but that different components of the landscape to a different degree reflect, absorb or generate electromagnetic radiation.

The informative materials obtained by methods for electromagnetic sounding of the earth provide data on many geological objects lying at different, sometimes extremely considerable depths. This applies, in particular, to faulted and folded structural forms forming as a result of tectonic movements. "The appearance ('showing through') of deep structures at the surface occurs due to its mechanical deformations associated with deformations of deeper layers and due to its geochemical transformations associated with ascending flows of gas-fluid products of the transformation of matter of deep layers in the earth's crust and upper mantle." [See: V. I. Makarov and L. I. Solov'yeva, "Crossed Structural Plan of the Earth's Crust and the Problem of Manifestation of its Deep Elements at the Surface (in the Example of the Tien Shan and the Transkaya Platform)," ISSLEDOVANIYE PRIRODNOY SREDY KOSMICHESKIMI SREDSTVAMI. GEOLOGIYA I GEOMORFOLOGIYA (Investigation of the Environment by Space Vehicles. Geology and Geomorphology), Vol 5, Moscow, 1976.] Simultaneously movements of masses of the earth's crust cause changes in the gravity, magnetic, heat and other physical fields in the earth. The local changes in these fields predetermine the corresponding redistribution (or reforming) of the landscape components and are becoming one of the principal reasons for their geochemical transformation. The

reaction of the landscape-forming processes to the mechanical movements and to the changes in physical fields arising in this case leads to the formation of specific landscape components (serving as indicators of deep structure) or to the appearance of local, sometimes scarcely noticeable anomalies in the structure of its background components. These indicators and anomalies ensure the representation of the peculiarities of deep structure of the earth's crust on remote sensing materials. [See: V. I. Gridin, "Some Problems in the Theoretical Validation of Aerogeological and Morphometric Methods," STRATIGRAFIYA, LITOLOGIYA I POLEZNYYE ISKOPAYEMYYE BSSR (Stratigraphy, Lithology and Minerals of the Belorussian SSR), Minsk, 1966; V. I. Gridin, "On the Problem of the Influence of Local Changes in the Earth's Physical Fields on the Nature and Intensity of Relief-Forming Processes (in the Example of the BSSR)," SOVREMENNYYE EKZOGENNYYE PROTSESSY (Modern Exogenous Processes), Kiev, 1968.]

The history of use of remote methods in petroleum exploration work, despite the relative newness of the entire direction of aerospace study of the earth's natural resources, is already characterized by definite successes.

Abroad, particularly in the United States, the extensive use of remote methods for seeking petroleum and gas deposits was already begun in the 1950's. At first use was made only of aerial photographic surveying -- on black-and-white, then on spectrozonal and color films. The global character of use of remote methods and the striving to increase their effectiveness have led to the use not only of the visible part of the spectrum, but also other ranges of electromagnetic oscillations. Radar, IR, radiothermal and other remote methods have appeared, without which topographic, geological engineering, magnetic, soil and other types of surveys would be unthinkable at the present time.

At the same time there has been development of complex systems for multispectral surveying, which necessitated spectrophotometric studies of the investigated features, and also determinations of its influence on the subsequent processing of remote sensing data. Television systems for continuous investigation of the earth with transmission of data through the radio channel at a real time scale began to be used extensively. The enormous volume of collected information made it necessary to develop and introduce means for the mechanization and automation of the processes of interpretation of information materials and also the training of specialists in the corresponding fields of specialization. The routineness in carrying out the entire complex of studies, the unquestionable economic effectiveness and other merits of remote methods are brought to our attention by a whole series of petroleum companies, which also finance a considerable part of the work on the United States space program.

In the Soviet Union aerial methods are being employed for the practical solution of problems in regional geology, and in particular, in a geological survey of unforested areas. Since 1966 aerial methods have become mandatory in geological surveying, geophysical and exploration work carried out by

organizations of the USSR Geology Ministry. In the Petroleum Industry Ministry system experimental-methodological aerogeological investigations were initiated in 1966-1968. They have been carried out under the direction of the Institute of Geology and Mineral Exploitation. The scientific plans of this institute -- as the key institute of the branch -- include the most important themes, fundamental for each of the directions in aerospace research, as well as those having general methodological importance. A considerable part of the investigations are carried out under joint programs which are coordinated with both the corresponding subdivisions of the Petroleum Industry Ministry and with the organizations and enterprises of the other ministries and departments. Such an organizational form proved to be most effective for the development of new remote methods and the introduction of their results.

The launching of the first artificial earth satellite, the first space flight of Yu. A. Gagarin, the first photographs of the earth from space, obtained by G. S. Titov, and the work of the first automatic and manned orbital stations in the Soviet Union opened up a new space era in study of the earth's natural resources. The development of the technical means for space photography ensured obtaining necessary photographs with a resolution satisfying the modern requirements on carrying out not only regional, but also detailed petroleum exploration work. The possibility was afforded for obtaining fundamentally new information and considerably rationalizing the process of study of petroleum- and gas-bearing regions. [See: NEFTEGAZONOSNOST' SSSR (OB"YASNITEL'NAYA ZAPISKA K KARTE NEFTEGAZONOSNOSTI SSSR MASSHTABA 1:2500000) (Occurrence of Petroleum and Gas in the USSR (Explanatory Commentary for the Map of Occurrence of Petroleum and Gas in the USSR at a Scale 1:2500000)), Moscow, 1976.]

"The Fundamental Directions in Development of the USSR National Economy in 1976-1980," adopted by the 25th Congress CPSU, called for a considerable broadening of the use of aerial high-altitude and space photography for a study of the earth's natural resources. In the implementation of the congress resolutions there has been an expansion of scientific research and experimental studies for creating new remote methods, their testing and introduction into practical petroleum exploration work.

Proceeding on the basis of the positive experience in use of remote sensing data obtained within the limits of the Pripyatskaya, Dneprovsko-Donetskaya and Ferganskaya petroleum and gas regions, the Petroleum Industry Ministry made provision for further improvement and introduction of remote methods for the search for petroleum deposits. For this purpose the ministry has organized a system of field specialized subdivisions in production combines. The task of these subdivisions is the carrying out of experimental-methodological and experimental-production investigations for the introduction of aerial and space methods under specific conditions prevailing in the studied regions.

The organization of the system of specialized subdivisions in the Petroleum Industry Ministry encountered definite difficulties caused by the shortage of specialists in the corresponding fields of specialization and skills, who are not specially prepared by colleges and technical schools. Permanently operating courses for increasing qualifications in aerospace methods have been established for the retraining of geologists and geophysicists. During the period 1976-1978 exercises were carried out in the prefield, field and office stages of the work for 63 specialists.

The aerospace service of the Petroleum Industry Ministry is carrying out a broad range of investigations. They include the development and testing of the methods and technology for remote study of petroleum- and gas-bearing regions applicable to solution of petroleum exploration problems; refinement of known and validation of new directions in geological studies for supporting the front of long-range search for petroleum deposits; refinement of the structure of known and detection of new areas for exploration with the formulation of specific recommendations for carrying out geophysical and drilling work. Scientific methods and technological procedures for remote sensing are used on an experimental basis by territorial specialized subdivisions of the ministry. At present the first results of such investigations and also materials from their checking by traditional geological-geophysical methods have been obtained for a number of petroleum- and gas-bearing provinces and oblasts. These materials make it possible to give a general evaluation of the geological and economic effectiveness of aerospace investigations carried out in our country in the search for petroleum.

The most representative results were obtained within the limits of the Dneprovsko-Pripyatskaya gas- and petroleum-bearing province. In overall-regional studies in collaboration with the "Priroda" State Center specialists prepared a map of the tectonic structure of the Pripyatsko-Dneprovsko-Donetskiy aulacogen (Fig. 1).

The structure of the northern and southern deep faults of this aulacogen was determined more precisely, as were regional longitudinal and transverse dislocations. As demonstrated by interpretation materials, the productive deposits of the zones of deep faults are collected into hemianticlinal folds. The petroleum exploration work carried out in the Ozeryanskaya, Prokopenkovskaya and other areas demonstrated that these folds can control industrial deposits of hydrocarbons. A comparison of data from remote sounding with the results of geological-geophysical investigations made it possible to formulate recommendations on carrying out petroleum exploration work in zones of deep faults.

The aulacogen is broken into large blocks by longitudinal and transverse faults. The total vertical amplitudes of neotectonic movements of the blocks attain 110-130 m. With an effective thickness of the productive horizons of several tens of meters these movements could exert a definite influence on reformation of deposits of hydrocarbons, which makes it possible to regard the neotectonic activity of the studied structural forms as one of the

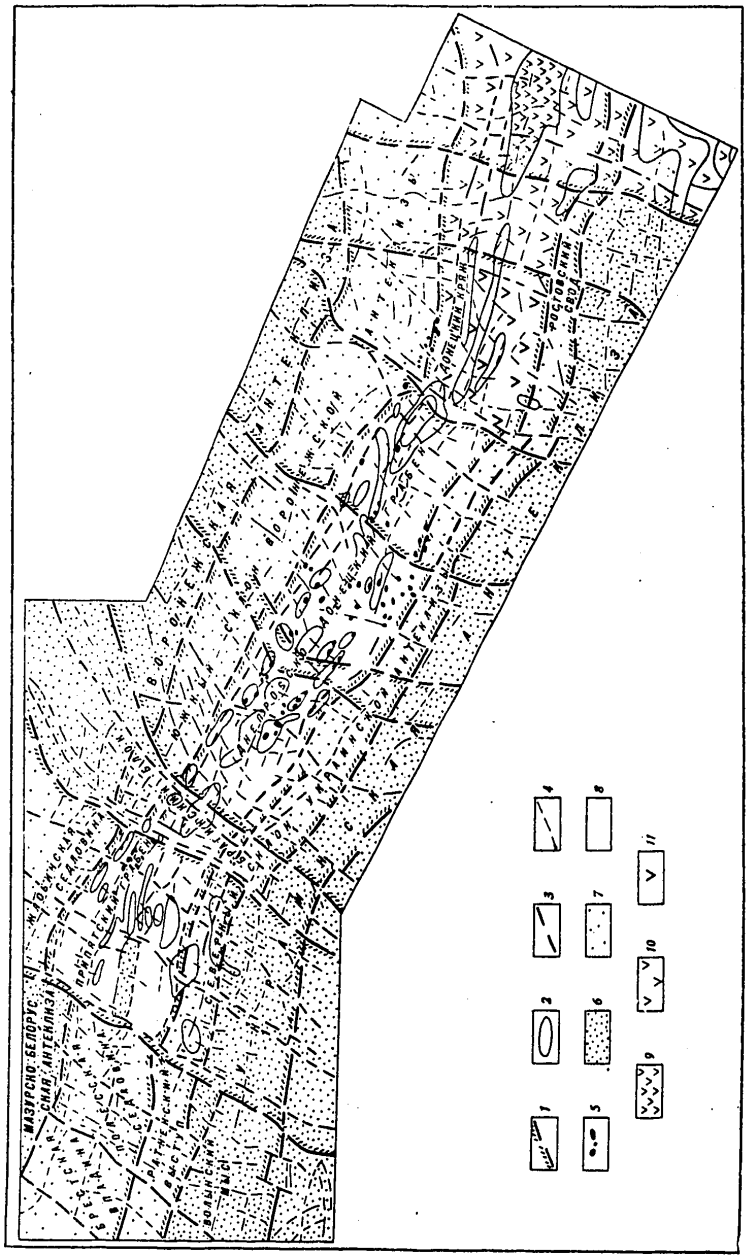

Fig. 1. Diagram of tectonic structure of Pripyatsko-Dneprovsko-Donetskiy aulacogen. Compiled on the basis of an interpretation of space photographs with use of a map of tectonic regionalization of the southern USSR (compiled by N. A. Yeremenko, V. I. Gridin, 1976). 1) outlines of major tectonic structures, 2) outlines of medium and small tectonic structures, 3) structural lines, expressed in structure of landscape and hypothetically comparable with zones of dislocations, 4) structural lines comparable with dislocations, 5) principal petroleum and gas deposits, 6) degree of plunging of basement or folded basement in "cores" of structural elements of pre-Baykalian age above 0, 7) 0-3 km, 8) 3-10 km, 9) degree of plunging of basement or folded basement in "cores" of structural elements of Hercynian age above 0, 10) 0-3 km, 11) 3-10 km.

---

criteria for evaluating the prospects of finding petroleum and gas. The macroblock structure of the Pripyatskaya petroleum-bearing region was confirmed and made more detailed when carrying out regional aerospace work. An analysis of these results in comparison with data from preceding and subsequent geological and geophysical investigations of the eastern half of the region will help in a more precise determination of the position and structure of already known uplift zones.

On the gently sloping slopes of these zones, and also in depression zones of the Pripyatskiy downwarp the use of aerospace methods made it possible to detect extensive zones of photoanomalies comparable with chains of hemianticlinal folds which are controlled by dislocations with a small amplitude. Thirty-one new zones of photoanomalies were detected. Thirteen were recommended for checking as being the most promising. Ten zones were checked by individual intersections and nine were confirmed.

On the basis of the results of multisided processing of remote and geological-geophysical data both longitudinal and transverse neotectonic zonality were detected in the Pripyatskiy downwarp. According to aerospace data, the longitudinal zones of neotectonic uplifts in general coincide with zones of productive horizons detected by seismic prospecting and drilling work. The transverse zones of neotectonic uplifts, bounded by dislocations of a northeasterly strike, were not detected by earlier geological-geophysical investigations. According to data from aerogeological investigations, transverse zones of uplifts in the neotectonic structural plan are seemingly superposed on longitudinal zones of uplifts. In the places of intersections of transverse and longitudinal zones there are local structures characterized by maximum amplitudes of the uplifts during the Neogene-Anthropogene. A comparison of the horizontal distribution of transverse zones of neotectonic uplifts with available factual data on the presence of petroleum indicates that all industrial petroleum deposits known at the present time are situated within the limits of the mentioned zones or their slopes. The detected regular correlation between the presence of petroleum and the peculiarities of neotectonic movements is based on a relatively small volume of factual material and requires further confirmation. But even now when defining

areas for priority petroleum exploration work and the distribution of such work it is necessary that transverse neotectonic zonality be taken into account.

Transverse dislocations and their zones are also of independent petroleum exploration significance. They separate local structures from one another and divide them into individual blocks. In particular, they separate the periclines of petroleum and gas deposits and in this case can serve as a tectonic shield of petroleum deposits. An example is the Ozeryanskoye uplift of the Dneprovsko-Donetskaya gas- and petroleum-bearing region, broken by transverse faults into a number of blocks. Figure 2 is a diagram of the structure of this area based on aerogeological data.

Due to the data which have been obtained it was possible to make more detailed the already known and to detect new promising directions in petroleum exploration work. Reference is to carrying out exploration in regions of anomalies associated with structural complications on the gently sloping monoclinal sides of uplift zones; periclines of petroleum and gas deposits cut by transverse faults; anomalies associated with structural forms in the zones of the Northern and Southern deep faults.

The good prospects for the mentioned directions were partially confirmed by subsequent seismic prospecting and drilling work.

The good results of detailed aerospace investigations in the Dneprovsko-Pripyatskaya gas- and petroleum-bearing province can be illustrated in the example of one of the sectors of experimental work situated in the northwestern part of the Dneprovsko-Donetskaya region. Figure 3 gives a comparison of the results of aerospace, preceding and subsequent geological-geophysical work in this sector.

The sector is situated within the limits of a region of well-developed petroleum production. It includes two petroleum and gas deposits. For a long time new areas promising for search for petroleum and gas deposits were not detected here by traditional geological-geophysical studies, but 13 local structures and their blocks to one degree or another promising for petroleum exploration were discovered. Aerospace investigations in the sector revealed photoanomalies corresponding to the mentioned search objects. All 13 known promising structures were represented on the materials from remote sensing with a total or at least a partial coincidence of outlines. In addition, 12 photoanomalies were detected. Definite patterns in the distribution of explorable structures were also detected: longitudinal and transverse zonality was noted and a significant role of dislocations of northwesterly and northeasterly strikes was established in the structure of the studied territory. Taking into account the mentioned patterns, six photoanomalies were recommended as priorities for subsequent petroleum exploration work.

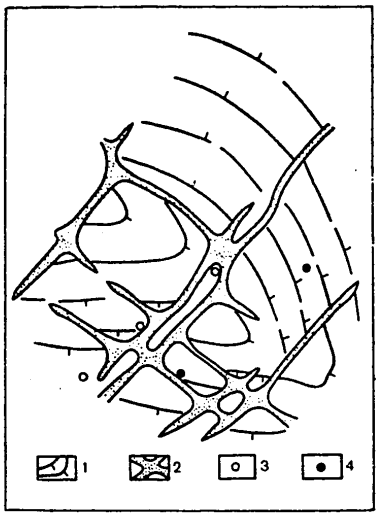

Fig. 2. Diagram of structure of Ozeryanskaya area according to aerogeological data. 1) structural lines expressed in structure of landscape and hypothetically associated with plicative dislocations, 2) surmised dislocations and their zones, 3) borehole not penetrating into productive strata, 4) borehole penetrating into productive strata

It was established by subsequent geological and geophysical work that nine of the eleven photoanomalies subjected to checking were associated with Carboniferous deposits and two anomalies were not confirmed by seismic prospecting data. Parametric and exploratory drilling was carried out within the limits of four photoanomalies. Petroleum and gas deposits were discovered in the Belousovskaya and Svetlichnaya anomalies. Gas flows and a core with petroleum were obtained in the Ozeryanskaya area using a stratum tester.

All the above enumerated facts indicate that even in regions exploited by the petroleum industry and characterized by considerable (although nonuniform) study, the combining of remote and traditional methods is creating a possibility for obtaining new information on deep structure, and on their basis refining the position of known explorable structures and with an adequately high degree of reliability detecting new ones.

The coefficient of confirmability of photoanomalies by subsequent geological-geophysical studies, judging from the results of work in the Dneprovsko-Pripyatskaya province, attains 0.8-0.9. Within the limits of the province, by aerospace investigations, the Institute of Geology and Mineral Exploitation has discovered 324 local anomalies. A total of 128 anomalies have been recommended as priority for checking, 54 have been drilled and 44 have been confirmed. As a result of the exploration and reconnaissance work in the checked photoanomalies it was possible to detect seven deposits and flows of gas and

petroleum were obtained in five areas. Thirteen areas were included in the drilling plan. Thus, the prospects are broadening for regions with a well-developed petroleum production and the most effective directions for subsequent geological prospecting work are noted.

Positive results with the use of remote methods in petroleum exploration work have also been obtained in other petroleum- and gas-bearing regions and oblasts.

Within the limits of the Bashkirskiy petroleum-bearing region on the slope of the Yuzhno-Tatarskiy arch and the Blagoveshchenskaya depression the aerogeological studies by the "BashNIPIneft'" institute along linearly oriented landscape components have defined zones of increased development of tectonic fissuring which serve as indicators of dislocations bounding Devonian graben-like downwarps and horstlike uplifts. As a result the possibility of a horizon-by-horizon structural interpretation was noted. A total of 30 new anomalies associated with local uplifts were detected. As a result of these investigations recommendations were given on the organization of seismic prospecting and drilling work.

In the Prikam'ye area, on the basis of the results of regional investigations of an aerogeological expedition of the "Permneft'" combine it was possible to make neotectonic and tectonic regionalization more detailed over an area of 55,000 km^2; extensive (up to 150 km) linearly oriented zones of photoanomalies, comparable with "seam" zones in the basement, were detected. By detailed work in the Solikamskaya depression near known petroleum deposits it was possible to detect 36 photoanomalies; in the southern part of the Verkhne-Pechorskaya depression -- 48 anomalies; in the zone of joining of the Verkhne-Pechorskaya and Solikamskaya depressions -- 21 anomalies. A network of structural boreholes was drilled in two anomalies. It was established that one anomaly corresponds to an uplift along the Lower Permian deposits, whereas another corresponds to a structural terrace.

In the West Siberian petroleum- and gas-bearing province the regional aerospace investigations carried out by the "Tyumenneftegeofizika" trust revealed the presence of linearly oriented photoanomalies associated with flexural-faulted zones. These postulated zones separate blocks which are considerable in size, characterized by a different direction and different amplitudes of movements in the neotectonic stage of geological development. On the basis of a comparison of the neotectonic regionalization map and available information on the presence of petroleum and gas in the studied territories there was found to be a regular relationship between the distribution of deposits of hydrocarbons and the peculiarities of neotectonic movements. The interpretation of materials from a specialized photographic survey within the limits of the Surgutskiy and Nizhnevartovskiy sectors demonstrated that most of the known petroleum and gas structures are reflected in the results of aerogeological mapping. In addition, 12 other anomalies were noted, hypothetically associated with local structures. Two of these anomalies were recommended for detailed seismic prospecting. The results of remote

investigations obtained in the Middle Ob' region are affording new prospects for finding petroleum and gas in this region.

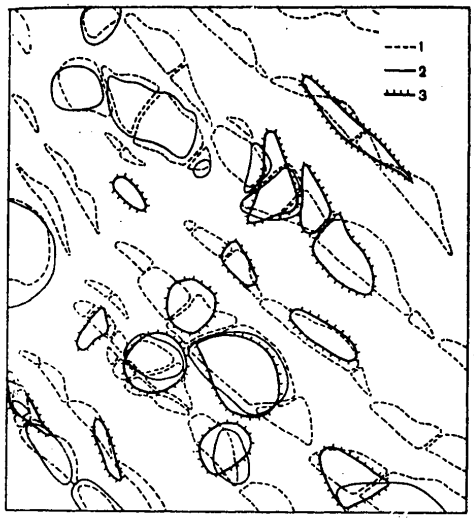

Fig. 3. Comparison of results of detailed aerospace, preceding and subsequent geological-geophysical investigations within limits of Dneprovsko-Donetskaya petroleum- and gas-bearing region. 1) outlines of photoanomalies detected by aerospace sounding methods, 2) outlines of local petroleum exploration areas detected by preceding geological-geophysical studies, 3) outlines of petroleum exploration areas detected by subsequent geological-geophysical work

In cooperation with the "Aerogeologiya" combine specialists compiled the "Cosmophototectonic Map of the Aral-Caspian Region," on the basis of which it was possible to carry out neotectonic, tectonic and petroleum geology regionalization of this territory. The principal directions in further exploration work in the Caspian depression, Ciscaucasia and the Mangyshlaksko-Buzachinskiy region were defined. [See: KOSMOFOTOTEKTONICHESKAYA KARTA ARALO-KASPIYSKOGO REGIONA (Cosmophototectonic Map of the Aral-Caspian Region), Moscow, 1978.]

The aerogeological investigations carried out by the "VolgogradNIPIneft'" institute, within the limits of the northern part of the Dono-Medveditskiy megarampart revealed 44 photoanomalies, in the northern part of the Privolzhskaya monocline -- 70, in the western part of the Caspian depression -- 53. Among these anomalies 84 were determined for the first time and 38 were recommended for the carrying out of geological exploration work. The fundamental possibility of using remote methods for detecting Upper Frasnian

reefs was demonstrated, which will considerably broaden the prospects for discovering deposits in traps of this type. It was also established that systems of dislocations detected by remote methods exert a decisive influence on the distribution of local structures, riftogenic formations and collectors of a high capacity of both the fissured and pore types. A borehole drilled with aerogeological data taken into account yielded a flow of petroleum from the Starooskol'skiy horizon of the Givetian stage with a depth of 4,686 m and thus a new deposit was discovered.

In the Fergana depression the aerospace investigations of the institute "SredazNIPIneft'" made possible a detailed study of tectonic regionalization. The position of longitudinal zones of dislocations was refined. The regularly constructed system of transverse faults and the transverse neotectonic zonality caused by them were detected. Regular correlations were established between the spatial distribution of deposits of hydrocarbons and the activity of structural forms in the Neogene-Anthropogene stage of geological development. Within the limits of the Naukatskiy downwarp, within the limits of the Bol'shaya Kyrkkol'skaya anticline it made possible a detailed description of the structure of zones of deep and regional faults; a number of new dislocations were detected; all faults were divided into three age generations. On the basis of the results of this work it was recommended that deep drilling be carried out in the Bol'shaya Kyrkkol'skaya anticline.

Within the limits of the Mangyshlakskava petroleum and gas region the regional studies of the "Mangyshlakneft'" combine made it possible to trace earlier known fault zones and detect new ones and a system of sublatitudinal and submeridional faults, determining the block structure of the territory, was defined. As a result of detailed studies a structural-tectonic diagram of the Rakushechnoye deposit was compiled.

Positive results of use of remote methods were also obtained within the limits of the Timano-Pechorskaya petroleum and gas province. By aerogeological methods it was possible to give a detailed description of the Kolvinskoye uplift, detected earlier by a geological survey; it became part of the structures prepared for exploratory drilling.

A generalization of the available materials makes it possible to conclude that aerospace investigations are of assistance in solving a whole series of petroleum exploration problems.

An overall-regional study of petroleum and gas basins will assist in inventorying and reinterpreting geological-geophysical materials on a basis common for the entire basin, in clarifying problems related to neotectonic and tectonic regionalization, in giving detailed descriptions of known and detecting new regional dislocations, in compiling overall-regional tectonic regionalization maps and maps of prediction of the presence of petroleum and gas to provide a scientific basis for subsequent geological prospecting studies and also for refining known and defining new directions in

petroleum exploration work for their long-term planning.

In regional geological-geophysical study of zones of petroleum and gas accumulation aerospace investigations favor the refinement of known concepts and the discovery of new peculiarities of modern structure, tectonic and neotectonic regionalization of zones of petroleum and gas accumulation; clarification of the peculiarities of geological development in the neotectonic stage and a comparative evaluation of the most recent activity of structural forms; determination and detailed description of the elements of fault tectonics and the mapping of regional tectonic fissuring; discovery and mapping of photoanomalies associated with zones of uplifts and major local structures; predicted evaluation of the studied territory and clarification of the directions, areas and volumes of priority petroleum exploration work.

In detailed petroleum exploration work remote sensing is helping to refine and make more detailed the structure of known areas for exploration with the formulation of recommendations for carrying out further exploration and reconnaissance work; to detect photoanomalies associated with promising exploration areas for preparing later geophysical methods for exploratory drilling; to evaluate exploration areas on the basis of their activity in the neotectonic stage and to designate which are priority for the carrying out of subsequent petroleum exploration work; to give a quite detailed description of known and detect new fault zones, local dislocations, zones of tectonic fissuring; to routinely analyze the results of geophysical and drilling work with subsequent issuance of recommendations on the siting of parametric and exploratory boreholes.

The preliminary results of experimental investigations make it possible to consider the use of aerospace methods to be promising both in the exploratory stage and in a number of cases also in the exploitation of petroleum deposits. Their use for topogeodetic and geological engineering support of reconnaissance and exploration work, development of oil fields, construction and operation of petroleum and gas pipelines, industrial and civil construction has gained general acceptance.

With respect to the method for determining the economic effectiveness of aerospace investigations carried out in the search for petroleum, for the time being it has not yet been developed. It is known that the average cost of the regional aerospace investigations carried out by the organizations of the Petroleum Industry Ministry per 1 km^2 is 17 rubles, and within the limits of one zone of photoanomalies -- 6,000 rubles; the cost of detailed aerospace work in an area of 1 km^2 is 58 rubles, and within the limits of one photoanomaly -- 2,700 rubles.

The aerospace service of the Petroleum Industry Ministry, in its scientific research and experimental aspects headed by the Institute of Geology and Mineral Exploitation, in general is well-organized and is successfully

functioning. The results of the scientific research and experimental work made it possible to recommend a number of methodological and technological developments for use. Their checking under experimental-field conditions has demonstrated that they yield excellent results and are highly effective.

5303
CSO: 1865

III. ARCTIC AND ANTARCTIC RESEARCH

Translations

UDC 551.324.433(99)+551.324.86

MONOGRAPH ON MELTING AND LIQUID RUNOFF FROM SURFACE OF THE ICE COVER IN ANTARCTICA

Leningrad TAYANIYE I ZHIDKIY STOK S POVERKHNOSTI LEDNIKOVOGO POKROVA ANTARKTIDY (Melting and Liquid Runoff from the Surface of the Glacier Cover in Antarctica) in Russian 1979 signed to press 21 Jun 79 pp 2, 127

[Annotation and table of contents from monograph by V. D. Klokov, Gidrometeoizdat, 128 pages]

[Text] The monograph gives the results of the latest investigations of the conditions for melting and liquid runoff on the periphery of the Antarctic continent. A considerable place is devoted to observations carried out in 1969/70 and 1972/73 in Enderby Land in the neighborhood of Molodezhnaya station. A method is proposed for determining the area of regions of liquid runoff. A study is made of the structure of the heat balance of the melting glacier cover. A quantitative evaluation is given of the liquid runoff from the surface of Antarctica. Recommendations are formulated on the reckoning and purposeful use of natural runoff for practical purposes with the onset of the socioeconomic development of Antarctica. The monograph is of interest for geographers, hydrologists, meteorologists and specialists interested in problems relating to heat and mass exchange in glaciers.

CONTENTS Page

[86-5303]

5303
CSO: 1865

-END-